

Review

Recent Developments in Metal-Based Catalysts for the Catalytic Aerobic Oxidation of 5-Hydroxymethyl-Furfural to 2,5-Furandicarboxylic Acid

Sohaib Hameed ^{1,2}, Lu Lin ¹, Aiqin Wang ¹ and Wenhao Luo ^{1,*}

¹ CAS Key Laboratory of Science and Technology on Applied Catalysis, Dalian Institute of Chemical Physics, Chinese Academy of Sciences, 457 Zhongshan Road, Dalian 116023, China; sohaibhameed@dicp.ac.cn (S.H.); linlu@dicp.ac.cn (L.L.); aqwang@dicp.ac.cn (A.W.)

² University of Chinese Academy of Sciences, Beijing 100049, China

* Correspondence: w.luo@dicp.ac.cn; Tel.: +86-411-8437-9738

Received: 23 December 2019; Accepted: 9 January 2020; Published: 15 January 2020



Abstract: Biomass can be used as an alternative feedstock for the production of fuels and valuable chemicals, which can alleviate the current global dependence on fossil resources. One of the biomass-derived molecules, 2,5-furandicarboxylic acid (FDCA), has attracted great interest due to its broad applications in various fields. In particular, it is considered a potential substitute of petrochemical-derived terephthalic acid (PTA), and can be used for the preparation of valuable bio-based polyesters such as polyethylene furanoate (PEF). Therefore, significant attempts have been made for efficient production of FDCA and the catalytic chemical approach for FDCA production, typically from a biomass-derived platform molecule, 5-hydroxymethylfurfural (HMF), over metal catalysts is the focus of great research attention. In this review, we provide a systematic critical overview of recent progress in the use of different metal-based catalysts for the catalytic aerobic oxidation of HMF to FDCA. Catalytic performance and reaction mechanisms are described and discussed to understand the details of this reaction. Special emphasis is also placed on the base-free system, which is a more green process considering the environmental aspect. Finally, conclusions are given and perspectives related to further development of the catalysts are also provided, for the potential production of FDCA on a large scale in an economical and environmentally friendly manner.

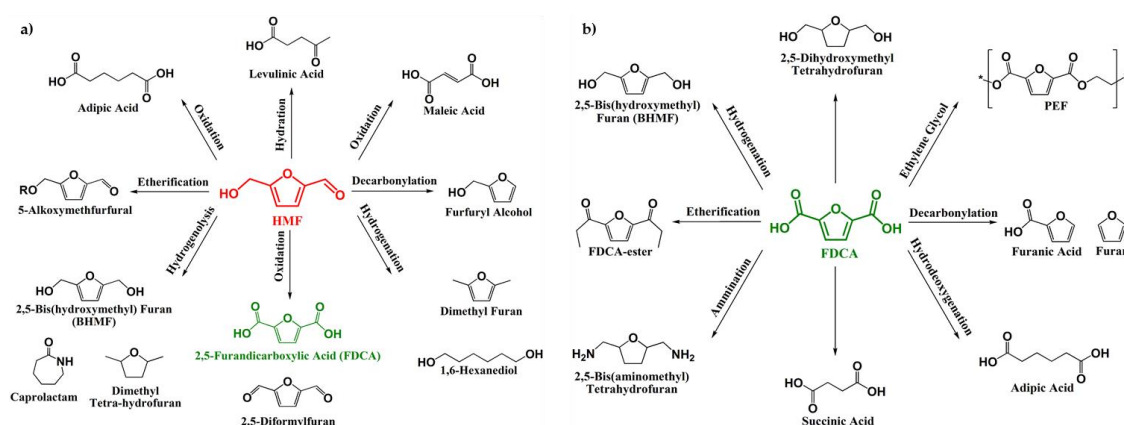
Keywords: biomass; 5-hydroxymethylfurfural; 2,5-furandicarboxylic acid; aerobic oxidation; metal catalysts

1. Introduction

The significantly growing demand for energy driven by an ever increasing global population and the strong economic growth in developing countries, the potential threats to the environment associated with the utilization of non-renewable fossil resources (oil, coal and natural gas) and difficulties with exploitation of the dwindling reserves have stimulated the research for alternative feedstocks that can be used for production of fuels and chemicals [1–5]. Biomass is one of the more promising and attractive alternative feedstocks, given its general abundance and wide-ranging availability in Nature and human society [1]. In addition, biomass is the only renewable carbon resource which can serve as a feedstock for the various carbon-containing chemicals and fuels that our society relies on [6].

5-Hydroxymethylfurfural (HMF), being a furan derivative, has been recognized as an important compound in our foods and as a versatile platform molecule derived from biomass for bulk chemicals and fuels production [7]. HMF can be used as biomass substrate compound for the production of

a plethora of end products such as biofuels, biodegradable plastics, additives, macromolecules and functional polymers via different reactions such as oxidation, hydration, hydrogenation, etherification and decarbonylation (Scheme 1a) [8,9]. In this review, we focus on one particular route, namely, the oxidation of HMF to a value-added chemical, 2,5-furandicarboxylic acid (FDCA). HMF can be produced from the dehydration of C₆ carbohydrates or direct transformation of cellulose, involving several steps including catalytic hydrolysis of cellulose to glucose, followed by isomerization of glucose to form fructose, and finally dehydration of fructose to produce HMF. Acid sites are normally required for the production of HMF, and the formation of a multitude of other components, i.e., formic acid, levulinic acid and humin, is also observed during the production of HMF, which hampers the purity and yield of HMF [10].

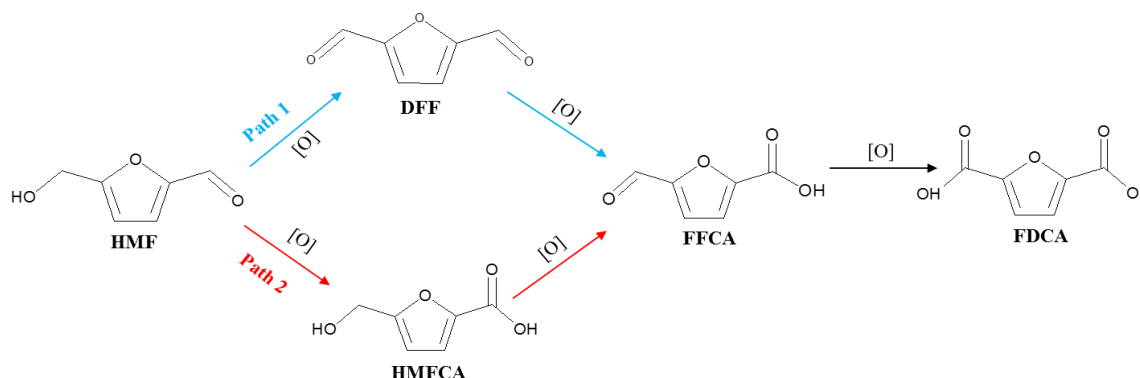


Scheme 1. Possible value-added platform chemicals from (a) HMF and (b) FDCA (reproduced from [11] with permission from Wiley-VCH, copyright 2019).

FDCA, being a promising molecule in the furan family, contains a multifunctional cyclic structure with two carboxylic acid groups attached at the *para* positions of the furan ring. It is listed on the top in all biomass-derived value-added chemicals by the US Department of Energy [12]. FDCA is considered stable, even at high temperatures, because of its high melting point (342 °C) due to which it is not easily soluble in common organic and inorganic solvents [13]. Scheme 1b summarizes the possible value-added chemicals which can be derived from FDCA in different reaction systems. FDCA is actually used as a starting material for the synthesis of a new class of bioderived polymers such as polyethylene 2,5-furandicarboxylate (PEF) [14,15]. PEF displays a series of excellent properties (thermal, chemical and mechanical resistance as well as easy depolymerization in Nature), compared to its petrochemical counterpart polyethylene terephthalate (PET) [16,17]. PET is the most common thermoplastic polymer material of the polyester family, and widely used in containers for foods and liquids, thermoforming for manufacturing, fibers for clothing, etc. [18]. The potential of substituting PET by this new bio-polyester PEF has stimulated great research efforts on this topic [19–22].

The production of FDCA has been studied since the 19th century. Firstly in 1876, Fittig et al successfully prepared FDCA by conducting the dehydration reaction of mucic acid over an acidic catalyst [23]. Concisely, aqueous hydrobromic acid (HBr) which acts both as catalyst and solvent was reacted with mucic acid to produce FDCA. Later, different dehydrating agents were also applied, along with some modifications to get higher efficiency in the dehydration process but this process is limited because of the severe reaction conditions i.e., high temperature (>120 °C), >20 h reaction time, the use of highly concentrated acids and less FDCA selectivity as well as moderate yield (<50%) [24]. Later HMF emerged as a promising biomass feedstock to produce FDCA. Direct oxidation of HMF is a simple method for the efficient and economical production of bio-based FDCA. Scheme 2 presents the general reaction scheme for the production of FDCA by catalytic oxidation of HMF monomer. In the typical reaction pathway, the synthesis of FDCA through catalytic oxidation of HMF proceeds initially through the selective oxidation of the hydroxyl group of HMF to produce 2,5-diformylfuran

(DFF) (Scheme 2, Path 1), or via oxidation of the aldehyde group to form 5-hydroxymethyl-2-furan carboxylic acid (HMFCFA) (Scheme 2, Path 2). Both intermediates are then further oxidized to 5-formyl-2-furancarboxylic acid (FFCA), which is finally transformed to FDCA [25]. Several reaction systems with different oxidants are used to activate the oxygen species for catalytic oxidation of HMF such as oxygen, air, H₂O₂, and KMnO₄ [26]. Oxygen or air are normally preferred for HMF oxidation due to the broad availability, low price, and benignity to the environment.



Scheme 2. Reaction scheme for catalytic oxidation of HMF into FDCA.

Figure 1 depicts the total number of research publications on HMF and FDCA per year from 2000 to 2019. The past few years in particular have seen a significant increase in the number of publications on HMF and FDCA chemistry. Due to maximum product separation capability, oxidation of HMF is considered as advantageous process to produce FDCA in an economical way [27].

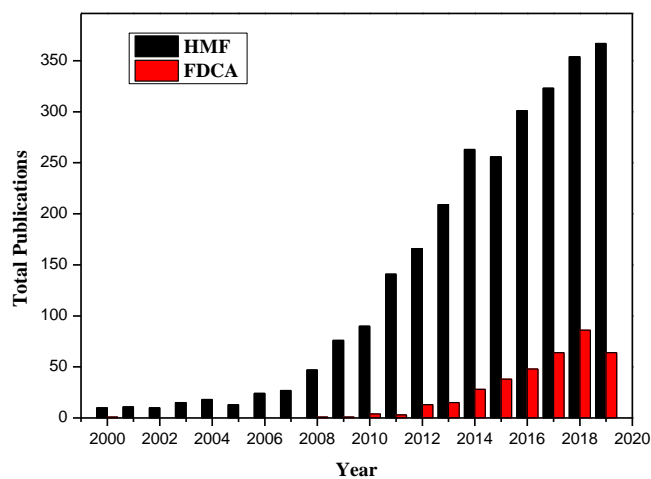


Figure 1. Total number of reported publications on HMF and FDCA chemistry per year from 2000 to 2019 (topic keywords searched in *Web of Science*: “5-hydroxymethylfurfural HMF” and “2,5-furandicarboxylic acid FDCA”).

Various catalytic systems involving heterogeneous catalysts [28], homogeneous catalysts [29], and bio-catalysts [30] have been reported for this process in aqueous media as well as organic and biphasic systems [31]. Electrochemical [32] and photocatalytic [33] processes have also been studied for HMF oxidation to FDCA. Owing to the good recycling capability and stability, heterogeneous catalysts are the most studied for this process. In this review, only metal-based solid catalysts will be discussed, which thus excludes the other catalytic systems, i.e., homogeneous catalysts and bio-catalysts. We first highlight the recent developments and current state of art of the application of metal-based heterogeneous catalysts for the catalytic aerobic oxidation of HMF to FDCA. The emphasis of this

review is thus put on comparing the catalytic performance of different catalysts categorized by metal, with specific examples using molecular oxygen (O_2) as oxidant and without using base additives. Reaction mechanisms of the aerobic oxidation of HMF to FDCA are also demonstrated in detail. Finally, conclusions are provided and perspectives referring to further development of the catalysts for the practical production are also highlighted, especially in designing efficient catalysts for green and cost-effective catalytic oxidation of HMF to FDCA.

2. Noble Metal Catalysts for FDCA Production

Oxidation can be catalyzed by metal sites in heterogeneous catalysis. Various noble metals such as gold (Au), platinum (Pt), palladium (Pd), ruthenium (Ru), and rhodium (Rh) catalysts have been reported for the catalytic oxidation of HMF to FDCA. The choice of molecular oxygen (O_2) as oxidant offers advantages of availability and benignity to the environment, in accordance with the concept of “green chemistry”. As oxygen is not easy to activate, supported noble metal catalysts are the main heterogeneous catalysts used for the catalytic aerobic oxidation of HMF to FDCA. We will first summarize the recent advances in applying noble metal catalysts for the oxidation of HMF to FDCA under relatively mild conditions.

2.1. Au-Based Catalysts

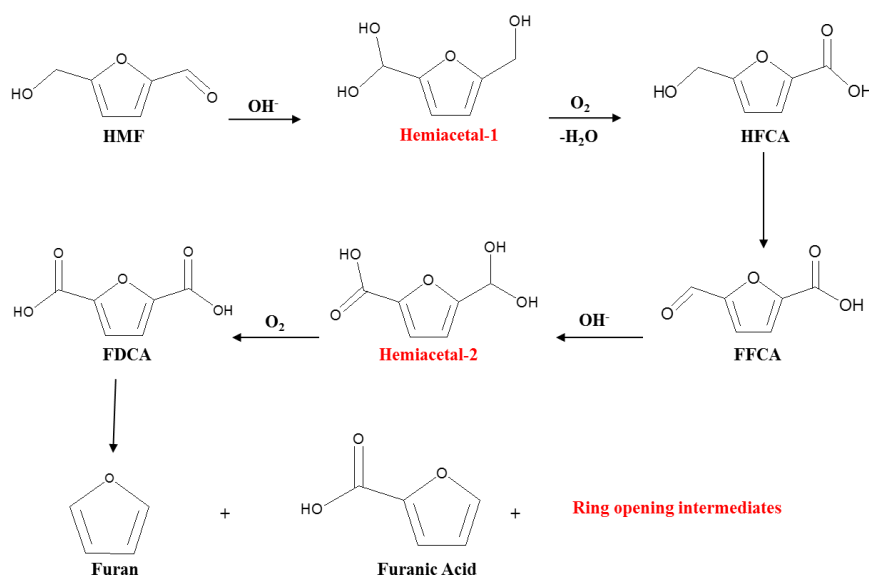
Gold (Au) was generally considered as inactive in the field of catalysis, but in the 1980s, it was a great achievement in research to discover the catalytic ability of Au, which opened a new gateway for researchers to develop highly active catalysts for many processes [34,35]. Recently, many catalysts are developed using Au that present promising catalytic performance for the aerobic oxidation of HMF to FDCA in aqueous solutions. The performance of different Au-based catalysts for catalytic aerobic oxidation of HMF to FDCA is summarized, and details are also given, in Table 1.

Table 1. Summary of reported results for the aerobic oxidation of HMF to FDCA over Au catalysts.

Catalysts	Base	Reaction Conditions			HMF Conv. (%)	FDCA Yield (%)	Ref.
		T (°C)	Oxidant P (bar)	Time (h)			
Au/CeO ₂	NaOH	130	Air, 10	8	100	>99	[36]
Au/TiO ₂	NaOH	130	Air, 10	8	100	>99	[36]
Au/Fe ₂ O ₃	NaOH	130	Air, 10	8	100	15	[36]
Au/C	NaOH	130	Air, 10	8	100	44	[36]
Au/m-CeO ₂	NaOH	70	O ₂ , 10	4	100	92	[37]
Au/CeO ₂	Na ₂ CO ₃	140	O ₂ , 5.0	15	>99	91	[38]
Au/TiO ₂	NaOH	30	O ₂ , 20	18	100	71	[39]
Au/HY	NaOH	60	O ₂ , 0.3	6	>99	>99	[40]
Au/TiO ₂	NaOH	60	O ₂ , 0.3	6	>99	85	[40]
Au/Mg(OH) ₂	NaOH	60	O ₂ , 0.3	6	>99	76	[40]
Au/CeO ₂	NaOH	60	O ₂ , 0.3	6	>99	73	[40]
Au/H-MOR	NaOH	60	O ₂ , 0.3	6	96	15	[40]
Au/Na-ZSM5-25	NaOH	60	O ₂ , 0.3	6	92	1	[40]
Au-Cu/TiO ₂	NaOH	95	O ₂ , 10	4	100	99	[41]
Au ₈ -Pd ₂ /C	NaOH	60	O ₂ , 30	4	>99	>99	[42]
Au/HT	Base free	95	O ₂ , 1	7	>99	>99	[43]
Au/HT-AC	Base free	100	O ₂ , 5	12	100	>99	[44]
Au-Pd/CNT	Base free	100	O ₂ , 5	12	100	94	[45]
Au-Pd/CNT	Base free	100	Air, 10	12	100	96	[45]
Au-Pd/CNT	Base free	100	O ₂ , 5	18	100	91	[45]
AuPd-nNiO ^a	Base free	90	O ₂ , 10	6	95	70	[46]
AuPd-La-CaMgAl-LDH ^b	Base free	100	O ₂ , 5	6	96.1	89.4	[47]

^a nNiO = nanosized NiO ^b La-CaMgAl-LDH = La doped Ca-Mg-Al layered double hydroxide.

The choice of support for Au-based catalysts can also have a great impact on the catalytic performance in HMF oxidation. When using TiO_2 and CeO_2 as supports, Au-based catalysts showed nearly quantitative FDCA yields of >99% at 65 °C under 10 bar of air after a reaction time of 8 h; in contrast, Au catalysts supported on carbon and Fe_2O_3 only afforded FDCA yields of 44% and 15% under the same conditions, separately [36]. According to the reaction mechanism discussed in this study, HMFCFA was observed as the only intermediate. As shown in Scheme 3, HMF was first oxidized to HMFCFA very fast via the formation of a hemiacetal-1 intermediate. Owing to the fact no FFCA was directly observed, the authors proposed that FFCA was transformed via the oxidation of HMFCFA was quickly transformed into FDCA through the production of a second intermediate product, hemiacetal-2. Compared to the one-pot reaction, substrate degradation was strongly diminished and the catalysts life increased by performing the reaction in two steps: first the oxidation of HMF into HMFCFA at a low reaction temperature of 25 °C and, second, the subsequent oxidation of HMFCFA in FDCA at 130 °C. Reductive pretreatment of the Au/ CeO_2 was shown to efficiently increase the catalytic activity due to increased amount of Ce^{3+} and oxygen vacancies. The increased Ce^{3+} species and oxygen vacancies on the support were shown to have a great effect on transferring hydride and activating O_2 during the oxidation of the alcohol group. The Lewis acid sites of Ce^{3+} centers and Au^+ species of Au/ CeO_2 could easily accept a hydride from the C–H bond in alcohol or in the corresponding alkoxide to form Ce–H and Au–H, with the simultaneous formation of a carbonyl species. The oxygen vacancies of CeO_2 could activate O_2 and form cerium-coordinated superoxide ($\text{Ce}-\text{OO}$) species, which subsequently evolved into cerium hydroperoxide by hydrogen abstraction from Au–H. The cerium hydroperoxide then interacted with Ce–H, producing H_2O and recovering the Ce^{3+} centers. Au–H donated H and changed back to the initial Au^+ species. Further improvement of activity of Au/ CeO_2 was reported by Lolli et al [37]. An ordered mesoporous CeO_2 (m- CeO_2) supported Au catalyst was synthesized by nanocasting technique using meso-structured silica SBA-15 as hard template. Au nano-particles immobilized on this high surface area mesoporous CeO_2 showed a FDCA yield of 92% with 100% HMF conversion under relatively mild reaction conditions ($T = 70$ °C, $P_{\text{O}_2} = 10$ bar, and $t = 4$ h).



Scheme 3. Reaction mechanisms for aerial oxidation of aqueous HMF over CeO_2 supported Au catalysts (reproduced from [36] with permission from Wiley-VCH, copyright 2009).

Formation of undesired humin is a great issue for HMF transformation, especially in concentrated HMF solutions. Kim et al. reported recently progress in utilizing Au/ CeO_2 catalyst for achieving 90–95% yield of FDCA via aerobic oxidation of acetal derivatives of HMF [38]. In this approach, protection of aldehyde group of HMF with 1,3-propanediol was proposed to prevent the formation of

undesired humin via decomposition and self-polymerization, and to achieve efficient FDCA yield from the resultant HMF acetal derivative. Even in concentrated solutions of 20% PD-HMF, FDCA could still be obtained in a high yield of 91% at 140 °C and 5 bar O₂, for 15 h reaction. This example presents a significant advance over the conventional oxidation of HMF that gives only reasonable FDCA yields in dilute solutions.

Zeolite-supported Au catalysts have also been investigated for the catalytic oxidation of HMF by Xu et al. [40]. The Au/H-Y catalyst showed high yield of FDCA (>99%) with a quantitative HMF conversion under mild reaction conditions (T = 60 °C, P_{O₂} = 0.3 bar and t = 6 h), which was much higher than that of Au supported on Mg(OH)₂, TiO₂, CeO₂, H-MOR, and ZSM-5. Further characterization indicated that Au-nanoclusters (approx. 1 nm) are encapsulated inside the supercages of the H-Y-zeolite, and the confinement of the supercage prevented the further agglomeration of Au nanoclusters into large particles (Figure 2). The interaction between the acidic hydroxyl groups in the zeolite supercage and Au clusters has been shown to be responsible for stabilization of the Au species, to which the high catalytic efficiency for the oxidation of HMF to FDCA was ascribed [40].

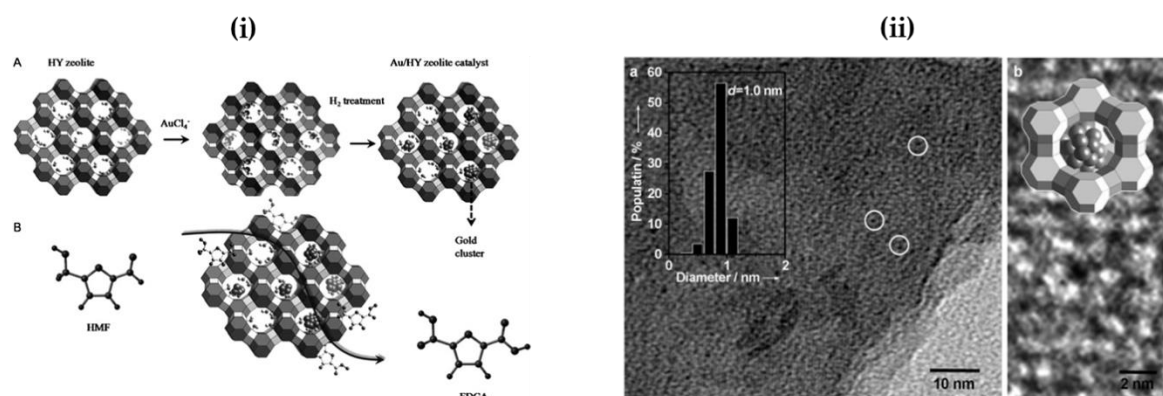


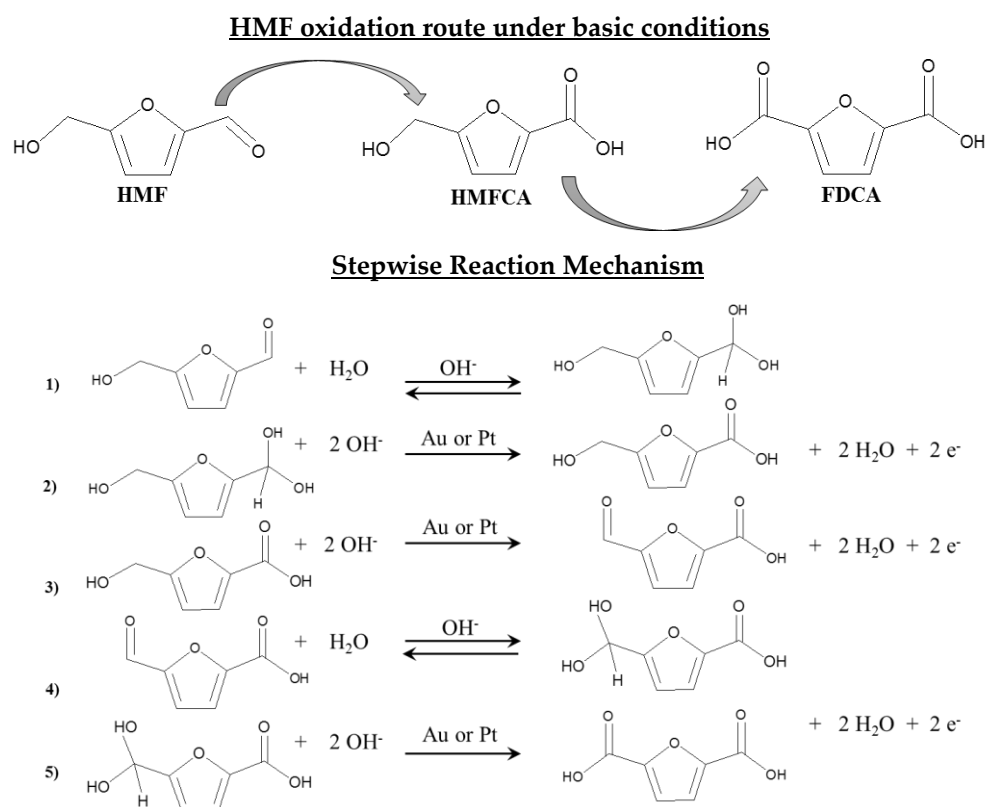
Figure 2. (i)-A Schematic illustration of synthesis for Au-nanoclusters in HY zeolite supercages (i)-B Catalytic oxidation process (ii)-a TEM image of Au/HY (ii)-b HR-TEM image of Au/HY (reproduced from [40] with permission from Wiley-VCH, copyright 2013).

Various Au-based bimetallic catalysts were also studied for the oxidation of HMF to FDCA. The physical and chemical characteristics of the prepared bimetallic catalysts can be simply tuned by altering catalytic composition, particle size and mixing equality. Pasini et al. reported that the Au-Cu/TiO₂ bimetallic catalyst afforded higher catalytic activity and stability over its corresponding mono-metallic Au/TiO₂ for HMF oxidation into FDCA [41]. All the bimetallic Au-Cu/TiO₂ catalysts with different Au/Cu mole ratio prepared via a colloidal route showed an improved activity, by at least factor of two compared to their corresponding monometallic Au catalysts. Under the optimal reaction conditions (10 bar O₂, 4 equiv of NaOH, 95 °C), HMF conversion of 100%, and FDCA yield of 99% were attained after 4 h (Table 1). The isolation of Au sites caused by AuCu alloying was the main reason for the excellent catalytic activity of the Au-Cu/TiO₂ catalysts for HMF oxidation into FDCA. The Au-Cu/TiO₂ catalyst could be easily recovered and reused without significant leaching and agglomeration of the metal nanoparticles. Thus, a strong synergistic effect was also evident in term of the catalyst stability and resistance to poisoning. Similar results in catalytic performance were also demonstrated for the Au-Pd/AC catalyst [42]. Alloying Au with Pd at molar ratio of 8:2 on carbon support significantly increased the catalyst stability and activity than the monometallic counterparts for the aerobic oxidation of HMF to FDCA. The Au/AC catalyst showed good product selectivity, but suffered with catalyst deactivation, with a drop in 20% of HMF conversion after the fifth run. No Au leaching from the catalyst was detected, and the deactivation was mainly attributed to irreversible adsorption of the byproducts or intermediates and the agglomeration of Au particles. In contrast, Au-Pd/AC delivered an excellent stability with a FDCA yield of 99% even after the fifth run.

The alloying of a second metal (e.g., Pd or Cu) with Au to form bimetallic alloy catalysts can indeed combine the advantages of different components and thus improve the catalyst performance.

To understand the strategic reaction mechanism and role of base, molecular oxygen and Au catalysts, Davis and co-workers studied the reaction route for oxidation of HMF to FDCA over Au/TiO₂ catalyst in alkaline medium (NaOH) using an isotope labeling approach [48,49]. By control experiments, base and a metal catalyst were shown to be important to produce FDCA at 22 °C. The aldehyde side-chain of HMF undergoes a rapid reversible hydration to a geminal diol through nucleophilic addition of a hydroxide ion to the carbonyl and subsequent proton transfer from water to the alkoxy ion intermediate (Scheme 4, step 1). This step is due to the incorporation of two ¹⁸O atoms in HMFCa when the reaction was performed in H₂¹⁸O. The second step is the dehydrogenation of the geminal diol intermediate, facilitated by the hydroxide ions adsorbed on the metal surface, to form the carboxylic acid HMFCa (Scheme 4, step 2). Further oxidation of the alcoholic group of HMFCa is required to produce FDCA. Base deprotonates the alcoholic group to form an alkoxy intermediate in solution [50]. Hydroxide ions on the catalyst surface then facilitate the activation of the C–H bond in the alcoholic group to form the aldehyde intermediate, 5-formyl-2-furancarboxylic acid (FFCA) (Scheme 4, step 3). The next two steps (Scheme 4, steps 4 and 5) oxidize the aldehyde function of FFCA to form FDCA. These two steps are expected to proceed similarly to steps 1 and 2 for oxidation of HMF to HFCA. The reversible hydration of the aldehyde group in step 4 to a geminal diol accounts for two more ¹⁸O atoms incorporated in FDCA when the oxidation is performed in H₂¹⁸O. Overall, complete HMF oxidation to FDCA illustrates that water molecules incorporate all four oxygen atoms in FDCA instead of readily available oxidant (O₂). The isotope labeling experiments of ¹⁸O₂ and H₂¹⁸O revealed that water was the source of oxygen atoms during the oxidation of HMF to HMFCa and FDCA, probably through direct participation of hydroxide in the catalytic cycle. Molecular oxygen was essential for the production of FDCA and played an indirect role during oxidation by removing electrons deposited into the supported metal particles. Those results provided a fundamental understanding of the roles of added base and molecular oxygen for FDCA production from HMF [49].

Most aerobic oxidations of HMF over Au catalysts are conducted in the presence of excess base, however, considering environmental and economic concerns, base-free HMF to FDCA oxidation systems are more desirable. Thus, some reports on the oxidation of HMF to FDCA over Au-based catalysts without using base were published recently. Gupta et al. reported a hydrotalcite-supported Au catalyst (Au/HT) for the oxidation of HMF into FDCA without using base [43]. An excellent yield of 99% FDCA was demonstrated at 95 °C under 1 bar O₂ in water after 7 h. Compared to Au deposited on neutral support or acidic SiO₂, limited activity was shown, indicating the essential need for basic sites on the catalyst. Although Au/MgO gave a FDCA yield of 21%, it was much lower than that of Au/HT. TEM revealed a much larger size of Au nanoparticles on MgO (>10 nm) than that of Au/HT (3.2 nm), which should be the main reason for the lower catalytic activity of Au/MgO. Although the authors claimed that Au/HT catalyst could be reused, Zope et al. observed a severe leaching of Mg²⁺ from HT over Au/TiO₂ catalyst and HT as solid base during the oxidation of HMF, owing to the chemical interaction between the basic HT and the formed FDCA [51]. Further improvement in catalyst stability by modified robust hydrotalcite and activated carbon supported Au catalyst (Au/HT-AC) was demonstrated under base-free conditions [44]. Physical milling of homemade hydrotalcite and commercial activated carbon was applied for catalyst preparation. The Au/HT-AC catalyst showed superior catalytic activity (FDCA Yield = 99.5%) at 100 °C, 5 bar O₂ pressure after 12 h of oxidation reaction (Table 1) with excellent catalytic stability (6 times). Availability of enough basic sites, large surface area of catalyst, and presence of hydroxyl and carbonyl groups are the reasons for enhanced catalytic performance and improved reusability.



Scheme 4. Expanded reaction pathway of HMF oxidation in basic (OH^-) media over Au or Pt catalysts (reproduced from [48,49] with permission from Royal Society of Chemistry & Elsevier, copyright 2012 and 2014).

Development of an active and stable bimetallic Au-Pd catalyst also reported by Wan et al [45]. A FDCA yield of 94% could be achieved at 100 °C and 0.5 MPa O_2 for 10 h, and a FDCA yield of 96% was obtained at 100 °C and 1 MPa air for 12 h. The surface carbonyl/quinone and phenol species on CNT was found to facilitate the adsorption of HMF and DFF, rather than FDCA, contributing to the high activity of the Au-Pd/CNT catalyst. In addition, the incorporation of Pd to Au/CNT changed the reaction pathway from HMFCFA to DFF route by facilitate the oxidation of the hydroxyl species of HMF, and further enhanced the oxidation of FFCA to FDCA, which is a difficult step for Au catalysts under base-free conditions. Notably, an improved stability with Au-Pd/CNT was also depicted, with marginal loss in activity during the consecutive six runs. Bonincontro et al. further reported an efficient and stable nNiO-supported Au-Pd alloy, with an optimal Au/Pd atomic ratio of 6:4, for base-free oxidation of HMF to FDCA [46]. A nearly quantitative yield of FDCA could be obtained at 90 °C after 14 h. NiO was shown to provide basic sites that can promote the reaction and the suitable choice of Au-Pd chemical composition favors the formation of FDCA. Gao et al. reported a highly efficient and stable bimetallic AuPd nanocatalyst over the La-doped Ca-Mg-Al layered double hydroxide (La-CaMgAl-LDH) support for base-free aerobic oxidation of HMF to FDCA in water [47]. A nearly full yield of FDCA could be achieved at 120 °C and 0.5 MPa O_2 after 6 h. No catalyst deactivation was observed at 100 °C and 0.5 MPa O_2 after four consecutive runs. The high dispersion of a small amount of La_2O_3 on the surface of LDH support were attributed to stabilize the support via preventing the deterioration of LDH support by formed carboxylic acid products during reaction, thus resulting in excellent stability and recyclability of AuPd/La-CaMgAl-LDH catalyst.

2.2. Pt-Based Catalysts

Pt-based catalysts were initially reported to be efficient for the aerobic oxidation of HMF to produce FDCA. Recent results of the aerobic oxidation of HMF to FDCA over Pt-based catalysts are summarized in Table 2. Verdeguer et al. studied the carbon supported Pt catalysts for the oxidation of HMF [52]. The addition of Pb into the Pt/C catalyst could improve the catalytic performance with a high FDCA yield of 99%, than that with the Pd/C catalyst (81%) at ambient conditions for 2 h (25 °C, P = 1 bar, a O₂ flow rate of 2.5 mL/s and 1.25 M NaOH solution). HMFCFA was detected as the reaction intermediate, pointing to the preferred oxidation of aldehyde group of HMF with Pt-Pb catalyst. Moreover, the addition of Bi to the Pt/C catalyst also showed a beneficial effect on the FDCA yield (Table 2) [53]. An optimal Pt/Bi molar ratio of about 0.2 showed a high FDCA yield of 98% for the Pt-Bi/C at 100 °C, 40 bar air and the use of four equivalents of NaHCO₃ after 6 h, compared to 69% for Pt/C catalyst. Both HMFCFA and DFF were detected as intermediates, and the oxidation of FFCA was figured out to be the rate-determining step for this Pt-Bi/C catalyst. Introducing Bi into the Pt/C catalyst improved the catalyst stability, owing to depressing the oxygen poisoning and leaching of Pt. Similar effect was also observed in another study over TiO₂ supported Pt-Bi catalyst [54].

Table 2. Results of the aerobic oxidation of HMF to FDCA over Pt-based catalysts.

Catalysts	Base	Reaction Conditions			HMF Conv. (%)	FDCA Yield (%)	Ref.
		T (°C)	Oxidant P (bar)	Time (h)			
Pt/C	NaOH	25	O ₂ , 1	2	100	81	[52]
Pt-Pb/C	NaOH	25	O ₂ , 1	2	100	99	[52]
Pt/C	Na ₂ CO ₃	100	Air, 40	6	99	69	[53]
Pt-Bi/C	Na ₂ CO ₃	100	Air, 40	6	100	>99	[53]
Pt/TiO ₂	Na ₂ CO ₃	100	Air, 40	6	90	84	[54]
Pt-Bi/TiO ₂	Na ₂ CO ₃	100	Air, 40	6	>99	99	[54]
Pt/Al ₂ O ₃	Na ₂ CO ₃	75	O ₂ , 1	12	96	96	[55]
Pt/ZrO ₂	Na ₂ CO ₃	75	O ₂ , 1	12	100	94	[55]
Pt/C	Na ₂ CO ₃	75	O ₂ , 1	12	100	89	[55]
Pt/CeO ₂	Na ₂ CO ₃	75	O ₂ , 1	12	100	8	[55]
Pt/TiO ₂	Na ₂ CO ₃	75	O ₂ , 1	12	96	2	[55]
Pt/Ce _{0.8} Bi _{0.2} O _{2-δ}	NaOH	23	O ₂ , 10	0.5	100	98	[56]
Pt/CeO ₂	NaOH	23	O ₂ , 10	0.5	100	20	[56]
Pt/RGO ^a	NaOH	25	O ₂ , 1	24	100	84	[57]
Fe ₃ O ₄ @C@Pt	Na ₂ CO ₃	90	O ₂ , 1	4	100	100	[58]
Pt/Al ₂ O ₃	pH = 9	60	O ₂ , 0.2	6	100	99	[59]
Pt/ZrO ₂	Base free	100	O ₂ , 4	12	100	97.3	[60]
Pt/C-O-Mg	Base free	110	O ₂ , 10	12	>99	97	[61]
Pt/C-EDA-x ^b	Base free	110	O ₂ , 10	12	100	96	[62]
Pt-Ni/AC	Base free	100	O ₂ , 4	15	100	97.5	[63]
Pt-PVP-GLY ^c	Base free	80	O ₂ , 1	24	100	94	[64]
Pt-PVP-NaBH ₄	Base free	80	O ₂ , 1	24	100	80	[64]
Pt-PVP-EtOH	Base free	80	O ₂ , 1	24	100	75	[64]
Pt-PVP-H ₂	Base free	80	O ₂ , 1	24	100	19	[64]
Pt-NP-Cl ^d	Base free	80	O ₂ , 1	6	100	65	[65]
Pt-NP5 ^e	Base free	80	O ₂ , 1	6	100	60	[65]

^a RGO = Reduced Graphene Oxide ^b EDA = ethylenediamine ^c PVP = polyvinylpyrrolidone. ^d NP-Cl = Nanoparticle with Cl ionic polymer ^e NP5 = Nanoparticle with C₁₂H₂₃O₂ ionic polymer.

The catalytic performance of different Pt-based catalysts is highly dependent on the choice of support. Ramakanta et al. compared the performance of different metal oxide-supported Pt catalysts under 75 °C, 1 bar O₂ and the use of Na₂CO₃ after 12 h. Pt catalysts supported on the non-reducible oxides (ZrO₂, Al₂O₃ and C) showed high FDCA yields of above 90%, while Pt catalysts supported on reducible oxides (TiO₂ and CeO₂) separately gave poor FDCA yields of 2% and 8% [55]. The authors attributed the higher catalytic performance on Pt catalysts to the lower oxygen storage ability of the non-reducible oxides, which could efficiently prevent the oxidation of active metal sites. Addition of Bi into the CeO₂ support could also enhance the catalytic performance of Pt/CeO₂ [56]. Pt-catalysts

with bismuth (Bi) modified ceria support, the Pt/Ce_{0.8}Bi_{0.2}O_{2-δ} afforded a FDCA yield of 98% while the Pt/CeO₂ only showed a FDCA yield of 20 % at 23 °C, 10 bar O₂. Moreover, the Pt/Ce_{0.8}Bi_{0.2}O_{2-δ} catalyst showed a good catalyst stability, and could be reused for five runs with a marginal loss of its FDCA yield (from 98% in the first run to 97% in the fifth run). In this work, Pt nanoparticles were believed to first react with the hydroxyl group of HMF and form the Pt-alkoxide intermediate, which was further converted to aldehyde by β-H elimination. Bi-containing ceria contained a large amount of oxygen vacancies, which could further promote the oxygen reduction process and the cleavage of the peroxide intermediate by bismuth. Therefore, the surface electrons were used to the reduction of oxygen, and a new catalytic cycle could be smoothly continued.

Carbon materials are widely used as catalyst supports owing to their good properties and easy availability. Apart from the most used active carbon, reduced graphene oxide (RGO) can be also used as support owing to its abundant surface functional groups, which can be used to anchor the metal nanoparticles. Niu et al. studied a series of RGO supported metal nanoparticles for the oxidation of HMF at 25 °C and 1 bar O₂, with the presence of NaOH and an O₂ flow rate of 50 mL/min [57]. The Pt/RGO catalyst showed a higher FDCA yield than Pd/RGO, Ru/RGO and Rh/RGO, and a FDCA yield of 84% could be obtained after 24 h. During the recycling experiments, an increase in HMFCa and a decrease in FDCA yield could be observed. Similar results that the Pt/C outperforms in catalytic activity than the Pd/C was also reported by Davis et al. [66]. Notably, Zhang et al. prepared a series of novel Fe₃O₄@C@Pt catalysts containing super-paramagnetic Pt-nanoparticles with a core-shell structure, and used for the oxidation of HMF (Figure 3) [58]. These novel Fe₃O₄@C@Pt catalysts have a spherical shape with a Fe₃O₄ core, a protective amorphous carbon shell and Pt nanoparticle clusters decorated on the surface. The preparation temperature showed an impact on the morphology of active Pt on the carbon shell (Figure 3i). The 110-Fe₃O₄@C@Pt prepared at reflux of 110 °C afforded a nearly full FDCA yield at 90 °C after 4 h during the oxidation of HMF (Figure 3ii). In addition, this catalyst can be reused up to three times without significant loss in performance. Platinum on alumina is also studied in basic conditions (pH = 9) and high FDCA yield (99%) is reported due to strong metal-substrate interaction through π-electrons of furan nucleus [59].

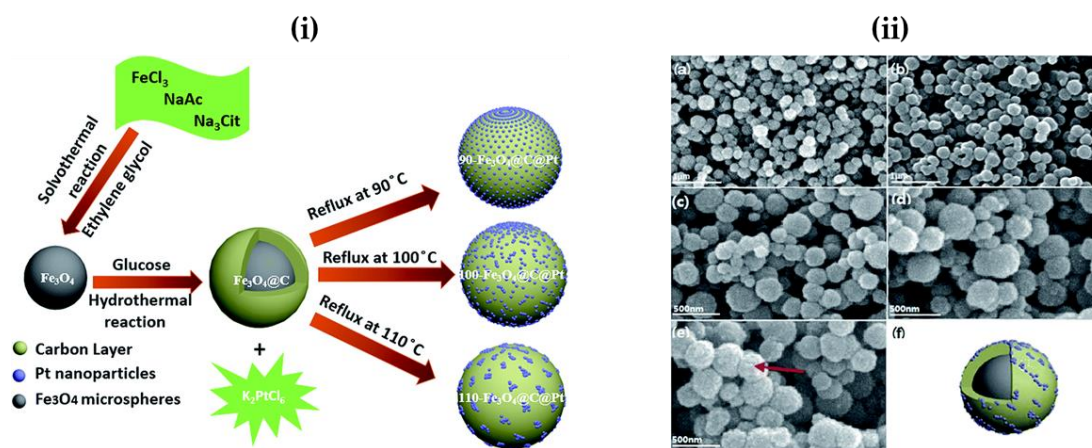


Figure 3. (i) Schematic illustration of synthesis of core-shell structure X-Fe₃O₄@C@Pt super-paramagnetic microspheres (X = Refluxing Temperature) (ii) (a) SEM images and model of 110-Fe₃O₄@C@Pt microspheres, (b) core/shell microspheres after coating with an amorphous carbon layer, and Pt-decorated magnetic core/shell microspheres: (c) 90-Fe₃O₄@C@Pt (d) 100-Fe₃O₄@C@Pt and (e) 110-Fe₃O₄@C@Pt synthesized at different temperatures. (f) A model image of a 110-Fe₃O₄@C@Pt microspheres (reproduced from [58] with permission from the Royal Society of Chemistry, copyright 2016).

Most of the above examples of the aerobic oxidation of HMF over Pt catalysts are generally performed in the presence of excess base. The disadvantages of basic feeds are that product solutions

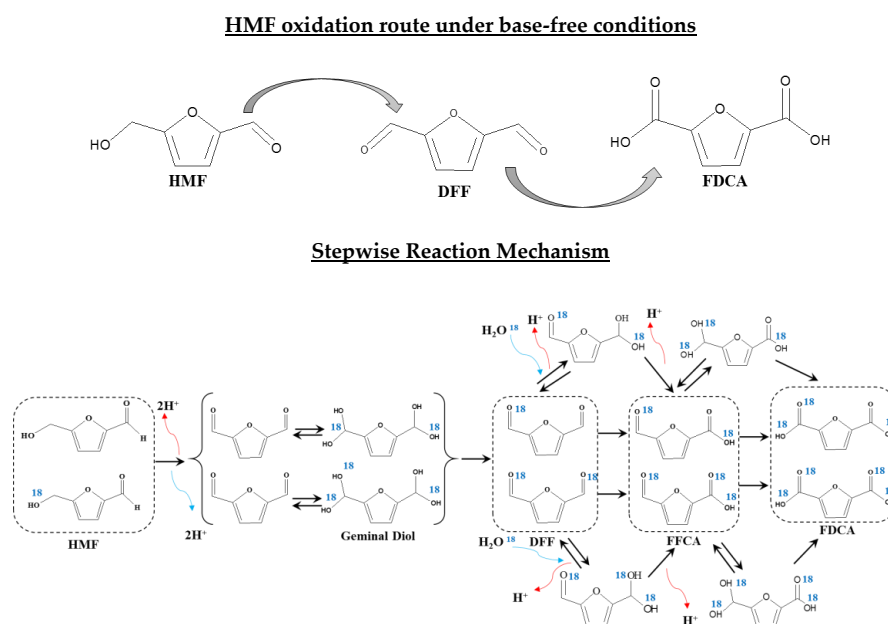
require neutralization of the base, and separation of the resulting formed inorganic salts. Base-free catalytic oxidation of HMF to FDCA has also been reported over Pt-based catalysts. Recently, Chen et al. prepared a Pt/ZrO₂ by the atomic layer deposition (ALD) method and conducted the aerobic oxidation of HMF under base-free conditions [60]. A complete HMF conversion and a FDCA yield of 97.3% under mild reaction conditions (100 °C, O₂, 4 bar, 12 h) were reported. The highly dispersed and uniform particle size of Pt particles was visualized by TEM. An improved C=O adsorption on the catalyst surface was also indicated by temperature programmed desorption of CO (CO-TPD), pointing to a strong interaction between reactants/intermediates. Both factors were attributed to the good catalytic activity for the Pt/ZrO₂. Han et al. designed a novel Pt catalyst with modified C-O-Mg support for base-free aerobic oxidation of HMF to FDCA [61]. A high FDCA yield of 97% could be obtained at 110 °C and 10 bar O₂. In addition, this catalyst could be used for ten times with little loss of activity. Even scaling up the reaction by 20 times at a large scale, a decent yield of isolated FDCA could achieve 74.9% with a high purity of 99.5%. Han et al. further developed a N-doped carbon- supported Pt for base-free aerobic oxidation of HMF to FDCA [62]. The synthesized Pt/C-EDA-x catalyst (where EDA = ethylenediamine and x = nitrogen dose) prepared by using EDA as nitrogen source showed higher catalytic activity than the counterparts using N,N-dimethylaniline (DMA), ammonia (NH₃), and acetonitrile (ACH) as nitrogen source. A FDCA yield of 96% was achieved with the Pt/C-EDA-4.1 catalysts at optimal conditions (T = 110 °C, P_{O₂} = 1 bar, and t = 12 h). This high catalytic performance is attributed to the formation of a new kind of medium basic site due to the formation of pyridine-type nitrogen in the catalyst.

Limited examples of Pt-based bimetallic catalysts are reported for base-free aerobic oxidation of HMF to FDCA. Shen et al. prepared a Pt-Ni/AC bimetallic catalyst by atomic layer deposition of Pt nanoparticles on the surface of Ni/AC for base-free oxidation of HMF to FDCA [63]. The bimetallic Pt-Ni/AC catalyst showed a higher activity (a FDCA yield of 97.5% yield with 100% HMF conversion) even with only a 0.4 wt % Pt loading at 100 °C and 4 bar O₂ after 15 h, compared to the monometallic counterparts with a higher Pt loading (the 5.6 wt% Ni/AC and 1.6 wt% Pt/AC). In addition, the bimetallic catalyst afforded good reusability for at least four 15 h runs without any obvious loss of catalytic activity. The authors proposed that the addition of Ni to Pt improved the ability of Pt for C=O adsorption and oxidation, thus increasing the activity of the Pt catalyst.

Pt nanoparticles stabilized by polymers were also shown to be effective for base-free aerobic oxidation of HMF to FDCA. Siankevich et al. reported that polyvinylpyrrolidone (PVP) stabilized Pt nanoparticles could promote the base-free aerobic oxidation of HMF into FDCA in water [64]. A high FDCA of 95% were achieved for the Pt-PVP-GLY catalyst at mild reaction conditions (T = 80 °C, P_{O₂} = 1 bar, and t = 24 h). Notably, a slight decrease of its catalytic activity was observed during five consecutive runs. The reaction mechanism was investigated for the Pt-PVP-GLY catalyst. Isotope (H₂¹⁸O) labeling technology was used to elaborate the reaction path, and mass spectrometric analysis of solutions after reaction verified the existence of ¹⁸O atomic levels. DFF and FFCA were detected as the reaction intermediates during this oxidation reaction, while HMFCFA was not detected during base-free oxidation of HMF.

As shown in Scheme 5, the aldehyde group was proposed to undergo a rapid reversible hydration to a geminal diol by nucleophilic addition of water, and followed by proton transfer to form DFF. Similar results were also reported by other researchers under base-free conditions at relatively low pH values [45,48]. The release of two protons from the hydroxyl group in HMF could form DFF. Mass spectrometric analysis of the reaction mixture confirmed that ¹⁸O was incorporated in the oxidation products (FDCA and FFCA). Peaks with *m/z* 161 and 163 were attributed to three and four ¹⁸O atoms incorporated in FDCA, and peaks with *m/z* 143 and 145 attributed to two and three ¹⁸O atoms incorporated in FFCA. Finally, a transfer of two H to the surface of the metal occurred to form the carboxylic acid groups, and molecular oxygen reacted with the surface hydride to release H₂O. Furthermore, Siankevich et al. reported Pt nanoparticles stabilized by an imidazolium-based cross-linked polymer (with chloride as the counter-anion), which could efficiently catalyzed the

oxidation of HMF to FDCA in water with oxygen as the oxidant under mild conditions ($T = 80\text{ }^{\circ}\text{C}$, $P_{\text{O}_2} = 1\text{ bar}$, and $t = 6\text{ h}$) [65]. Various counter-anion, that is, replacing chloride by BF_4^- , PF_6^- , bis(trifluoromethylsulfonyl)imide, hexanoate, or laurate anions, in the cationic polymer has been explored. The counter-anion indeed showed an impact on the structure of the obtained platinum nanoparticles, the surface electronic properties, and their catalytic activity. The highest reaction rates were obtained with the weakly nucleophilic bis(trifluoromethylsulfonyl)imide anion, which also favored Pt in the metallic state, leading to complete conversion of the substrate and a high yield of FDCA (65%).



Scheme 5. Reaction mechanism with inclusion of ^{18}O (blue). Main focusing units are boxed in dashed lines (reproduced from [64] with permission from Elsevier, copyright [2014]).

2.3. Pd-Based Catalysts

Pd-based catalysts also showed good catalytic performance for the aerobic oxidation of HMF into FDCA. According to the reported Pd-based catalysts for the aerobic oxidation of HMF, results along with their reaction conditions are summarized in Table 3.

Table 3. Summary of reported results for the aerobic oxidation of HMF to FDCA over Pd catalysts.

Catalysts	Base	Reaction Conditions			HMF Conv. (%)	FDCA Yield (%)	Ref.
		T ($^{\circ}\text{C}$)	Oxidant, P (bar)	Time (h)			
Pd/C	NaOH	23	O_2 , 6.9	6	100	71	[66]
Pd/ZrO ₂ /La ₂ O ₃	NaOH	90	O_2 , 1	6	>99	90	[67]
Pd/Al ₂ O ₃	NaOH	90	O_2 , 1	6	>99	78	[67]
Pd/Ti ₂ O ₃	NaOH	90	O_2 , 1	6	>99	53	[67]
Pd/PVP ^a	NaOH	90	O_2 , 1.01	6	>99	90	[68]
Pd/CC ^b	K ₂ CO ₃	100	O_2 , 20 mL/min	30	100	85	[69]
γ -Fe ₂ O ₃ @HAP-Pd ^c	K ₂ CO ₃	100	O_2 , 1	6	97	92.9	[70]
C-Fe ₂ O ₃ -Pd	K ₂ CO ₃	80	O_2 , 1	4	98.2	91.8	[71]
Pd/C@Fe ₂ O ₃	K ₂ CO ₃	80	O_2 , 1	6	98.4	86.7	[72]
Pd-Au/TiO ₂	NaOH	70	O_2 , 10	4	100	85	[73]
Pd/TiO ₂	NaOH	70	O_2 , 10	4	100	9	[73]
Pd-Au/HT ^d	NaOH	60	O_2 , 1	6	100	90	[74]
Pd/HT	NaOH	60	O_2 , 1	6	85	6	[74]
Pd-Ni/Mg(OH) ₂	Base free	100	Air	16	>99	89	[75]
Pd/HT	Base free	100	O_2 , 1	8	>99	>99	[76]

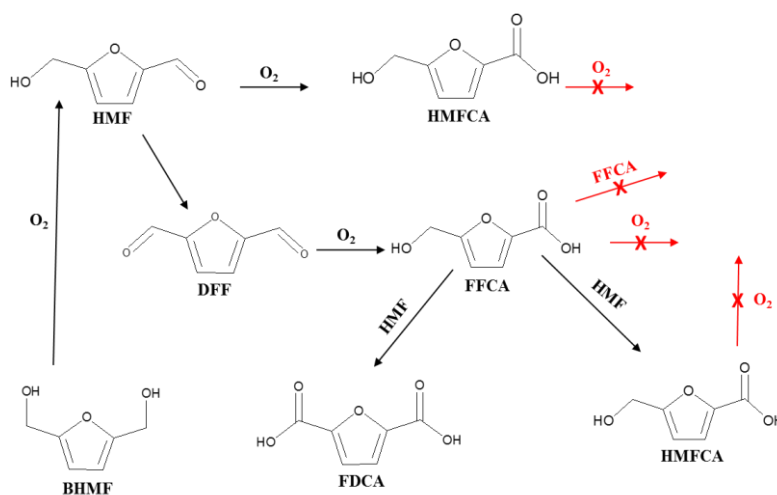
^a PVP = Polyvinylpyrrolidone ^b CC = Carbonaceous Catalyst ^c HAP = Hydroxyapatite ^d HT= Hydrotalcite.

The performance and particle size of different Pd-based catalysts are found to be dependent on the choice of the support. Siyo et al. studied the effect of catalytic support by depositing PVP stabilized Pd-nanoparticles on different metal oxide (Al_2O_3 , TiO_2 , $\text{KF}/\text{Al}_2\text{O}_3$, and $\text{ZrO}_2/\text{La}_2\text{O}_3$) supports in ethylene glycol with average particle size of 1.8 nm [67]. Pd/ $\text{ZrO}_2/\text{La}_2\text{O}_3$ catalyst showed to be a promising catalyst for HMF oxidation reaction, with a FDCA yield of 90% at 90 °C and 1 bar O_2 pressure after 8 h of reaction time (Table 3). TEM indicated that there was no obvious sintering of Pd nanoparticles in the spent Pd/ $\text{ZrO}_2/\text{La}_2\text{O}_3$ catalyst, whereas other catalysts showed serious aggregation. XPS confirmed that the majority of Pd remained as the metallic state and that the electronic structure of the Pd nanoparticles was unchanged in the spent Pd/ $\text{ZrO}_2/\text{La}_2\text{O}_3$ catalyst. The strong interaction between Pd nanoparticles and the metal oxide supports makes the catalysts more stable, to which its efficient catalytic performance is attributed. Siyo et al. further studied PVP stabilized Pd NP catalyst using ethylene glycol at three different Pd/NaOH ratios [68]. Differently sized Pd nanoparticles are obtained, with mean diameters between 1.8 nm and 4.4 nm, by changing the Pd/NaOH ratios. It was concluded that smaller Pd-nanoparticles showed higher FDCA yield. The highest FDCA yield obtained is 90% with greater than 99% HMF conversion over 1.8 nm Pd-nanoparticle catalyst synthesized with 1:4 molar ratio of Pd/NaOH [68]. These newly designed Pd-catalysts were able to store for long time (up to one month) in alkaline medium under ambient conditions without any change in their activity.

Owing to the ease in catalyst separation after its use, Zhang et al. prepared a Pd catalyst with magnetic properties [70]. In this catalyst hydroxyapatite (HAP) was layered on Fe_2O_3 using coating technique and Pd^{2+} ions are exchanged with HAP's Ca^{2+} ions with further reduction to produce Pd^0 nanoparticles. This novel catalyst showed excellent catalytic activity with almost 93% of FDCA yield and 97% HMF conversion under optimal reaction conditions ($T = 100$ °C, $P_{\text{O}_2} = 1$ bar, $t = 6$ h). This catalyst, due to its magnetic properties, is very easy to recycle as it can be easily separated using an external magnet without any change in catalytic activity. In another study, similar super paramagnetic catalyst was prepared by Mei and coworkers, in which graphene-based C- Fe_2O_3 -Pd catalysts were synthesized using reliable graphene oxide [71]. Pd nanoparticles and Fe_2O_3 particles are simultaneously deposited on surface of graphene oxide by one pot solvothermal technique. The reaction temperature and the base concentration notably affected the HMF conversion and FDCA selectivity. This carbon catalyst demonstrated high catalytic activity for oxidation reactions of HMF with FDCA with a yield of 91.8% and HMF conversion of 98.2% under mild reaction parameters (80 °C, O_2 , 1 bar, 4 h) with a base/substrate ratio of 0.5. The same research group further studied the Pd-based magnetic catalysts and effectively immobilized the Pd-nanoparticles on core-shell structure of C@ Fe_3O_4 (C acted as shell and Fe_3O_4 as core) with further reduction to generate Pd/C@ Fe_3O_4 catalysts [72]. In this technique, no excess reducing agents and capping reagents were used which makes it a clean and environmentally benign technique. Under optimal conditions, Pd/C@ Fe_3O_4 catalyst showed high catalytic activity in the aerobic oxidation of HMF to FDCA with 98.4% HMF conversion and 87.8% FDCA yield at 80 °C for 6 h reaction.

Bimetallic catalysts has also been studied and found to be an efficient approach for the aerobic oxidation of HMF to FDCA. Lolli et al. studied bimetallic Pd-catalysts for HMF oxidation to FDCA by preparing Pd-Au/ TiO_2 nanoparticle catalysts along with their monometallic counterpart Pd/ TiO_2 and revealed that minor alloying of Pd with gold (Pd:Au = 1:6) can enhance the FDCA yield from 9% to 85% with complete HMF conversion at 70 °C and 10 bar O_2 pressure for 4 h reaction [73]. Major reaction routes involved in FDCA production on pyrolyzed Pd-Au/ TiO_2 in the presence of base are summarized in Scheme 6. According to this study, once HMFCA is formed, the bimetallic catalyst showed a reaction route with no further oxidation due to the substantial inability of Pd and its alloy to oxidize the hydroxymethyl group of HMFCA [73]. FDCA molecule is produced via oxidation of alcohol part of the HMF molecule to produce DFF, which upon further oxidation gives FFCA. This produced FFCA has the options of producing FDCA or being oxidized to HMFCA which will again show the same behavior of no further oxidation. Recently, similar Pd-Au bimetallic catalysts were also synthesized on hydrotalcite (HT) support by Xia et al and their catalytic performance compared

with that of their monometallic counterparts Pd/HT and Au/HT catalysts [74]. High FDCA yield (up to 90%) was achieved over bimetallic Pd-Au/HT catalyst with Au:Pd = 4:1 at 60 °C and 1 bar O₂ pressure after 6 h of reaction. Similar to the previous report, the enhanced catalytic performance over a bimetallic catalyst is attributed to the synergistic effect between two metals and the formation of smaller particle size of the catalyst that facilitates the HMF oxidation reaction to produce FDCA. In addition, Gupta et al. further studied the bimetallic M_{0.9}-Pd_{0.1} (M = Ni, Co or Cu) alloy nanoparticles supported on in situ prepared Mg(OH)₂ for the aerobic oxidation of HMF to FDCA without using an external base additive [75]. Ni_{0.9}-Pd_{0.1}/Mg(OH)₂ was found to be the most efficient, and afforded superior catalytic activity with a FDCA yield of 89% compared to Co- or Cu-based bimetallic nanoparticles at 100 °C. The basicity of support could facilitate the activation of the hydroxyl group of HMF, leading to the enhanced FDCA production. Furthermore, Wang et al. reported another HT supported Pd nanoparticle catalyst in base-free environment, in which Mg-Al-CO₃ HT supported Pd catalysts are synthesized with different Mg/Al ratios [76]. The Mg/Al molar ratio 5:1 with 2% Pd metal loading (2%Pd/HT-5) appeared to be best in terms of catalytic activity due to formation of weak basic sites (OH⁻ groups). FDCA yields greater than 99% are achieved with >99% HMF conversion for 8 h under mild reaction conditions (T = 100 °C and P = 1 bar).



Scheme 6. Reaction pathways for HMF oxidation over Pd-Au/TiO₂ catalyst (reproduced from [73] with permission from Elsevier, copyright 2015).

2.4. Other Noble Metal Catalysts

The aerobic oxidation of HMF to FDCA can also be normally catalyzed with different Ru-based catalysts at moderate reaction temperatures ranging from 100–150 °C, with O₂/air pressure of 1 to 40 bar and base additives [77–83]. Majorly, Ru-based catalysts were reported for the oxidation of HMF to DFF in organic solvents [84]. While only a few examples were extended to the oxidation of HMF to FDCA in water [85]. The performance of different Ru-based catalysts, for catalytic aerobic oxidation of HMF to FDCA is summarized, and details are also given in Table 4.

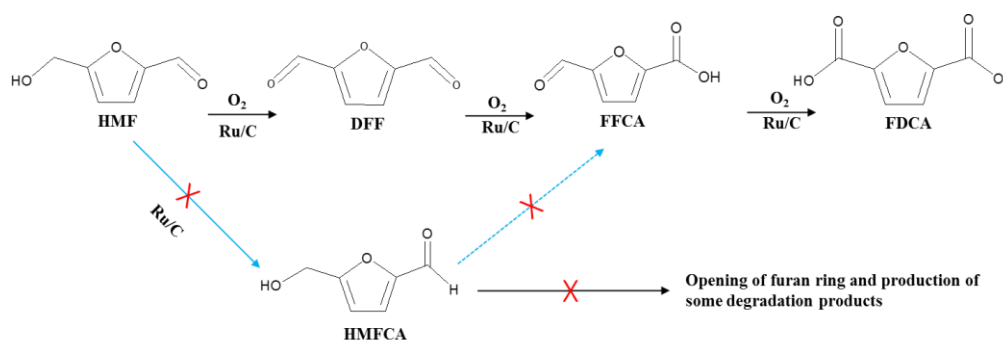
Yi et al. compared the effect of weak bases (K₂CO₃, Na₂CO₃, HT, and CaCO₃) with strong base (NaOH) over commercial Ru/C catalyst and concluded that the stronger base lead towards lower FDCA yield (69%) (Table 1) due to degradation of HMF at higher pH [78]. The weaker the base, the higher the FDCA yield. The maximum FDCA yield (95%) was attained by the use of CaCO₃ and FDCA obtained is in the form of its calcium salt because of its lower solubility.

Table 4. Summary of reported literature on HMF oxidation to FDCA over Ru catalysts.

Catalysts	Base	Reaction Conditions			HMF Conv. (%)	FDCA Yield (%)	Ref.
		T (°C)	Oxidant, P (bar)	Time (h)			
Ru/C	CaCO ₃	120	O ₂ , 2	5	100	95	[78]
Ru/C	Na ₂ CO ₃	120	O ₂ , 2	5	100	93	[78]
Ru/C	K ₂ CO ₃	120	O ₂ , 2	5	100	80	[78]
Ru/C	NaOH	120	O ₂ , 2	5	100	69	[78]
Ru/C	HT	120	O ₂ , 2	5	100	60	[78]
Ru/C	Base free	120	O ₂ , 2	10	100	88	[78]
Ru/C	NaHCO ₃	100	Air, 40	2	100	75	[79]
Ru/AC _{NaOCl} ^a	NaHCO ₃	100	Air, 40	4	100	55	[79]
Ru(OH) _x /La ₂ O ₃	Base free	100	O ₂ , 30	5	98	48	[80]
Ru(OH) _x /HT ^b	Base free	140	Air, 1	24	99	19	[80]
Ru/MnCo ₂ O ₄	Base free	120	Air, 24	10	100	99.1	[81]
Ru/CoMn ₂ O ₄	Base free	120	Air, 24	10	100	82.2	[81]
Ru/MnCo ₂ CO ₃	Base free	120	Air, 24	10	100	69.9	[81]
Ru/HAP ^c	Base free	120	O ₂ , 10	24	100	99.6	[82]
Ru/HAP ^c	Base free	140	O ₂ , 10	24	100	99.9	[82]
Ru/ZrO ₂	Base free	120	O ₂ , 10	16	100	97	[83]

^a AC_{NaOCl} = Activated Carbon oxidized with sodium hypochlorite ^b HT= Hydrotalcite ^c HAP = Hydroxyapatite.

In this reaction system, oxidation of HMF occurred through hydroxyl part rather than aldehyde part. Ru-catalyst favors the production of FDCA through DFF route instead of HMFC route due to oxidation of –OH group of HMF to –CHO group (Scheme 7). It is concluded that the conversion of –OH to –CHO is very fast step as compared to subsequent conversion of –CHO to –COOH, which is the rate determining step [78]. Over Ru/C catalyst, the oxidation of –CHO to –COOH is in less time (5 h) due to presence of base, which is a challenge in base-free conditions. This is why base-free reaction was carried out for relatively longer reaction time (10 h) to get 88% FDCA yield at similar reaction conditions (120 °C, O₂, 2 bar).



Scheme 7. Reaction route for oxidation of HMF to produce FDCA over Ru/C catalysts (reproduced from [78] with permission from the Royal Society of Chemistry, copyright 2016).

Kerdi and coworkers studied the modification of catalyst support using various doped carbons as supporting materials for Ru-based catalysts to investigate the consequence of surface properties as well as pore structure of carbon on oxidation rates [79]. Activated carbon was oxidized using sodium hypochlorite (NaOCl) and the Ru metal was impregnated on this oxidized AC_{NaOCl} support to prepare Ru/AC_{NaOCl} catalyst with particle size of 2 nm. Moderate results with FDCA yield of 55% with complete HMF conversion are obtained after 4 h reaction at 100 °C over a modified supported Ru catalysts [79].

Normally, the HMF oxidation reaction takes place in organic solvents or water, but this reaction is also investigated in ionic liquids (ILs) over Ru(OH)_x catalysts in base-free environment due to redox stability, negligible vapor pressure, non-flammability and unique dissolving abilities of ILs [80]. In this study, several different supports (TiO₂, Fe₂O₃, ZrO₂, CeO₂, HAP, HT, MgO, and La₂O₃) on Ru(OH)_x were tested along with various ILs. As shown in Table 4, Ru(OH)_x/La₂O₃ gives reasonable catalytic

activity, with a FDCA yield of 48% and high HMF conversion (98%) at 100 °C and elevated pressure (30 bar O₂). Ru(OH)_x/HT also appeared to be active in ILs with 99% HMF conversion but FDCA yield obtained is very low (19%) at high temperature (140 °C) and ambient pressure after 24 h of reaction. High temperature (140 °C) is selected to decrease the influence of viscosity of the mixture formed in ILs and catalyst [80]. As the idea for using ionic liquids is flopped because of their high cost, low FDCA yield and unfeasible large scale production, researchers continue to search for base-free phase oxidation over modified support Ru catalysts. In another work, MnCo₂O₄ spinel supported Ru-catalyst (Ru/MnCo₂O₄) with 4% metal loading shows an exceptionally high FDCA yield of 99.1% in comparison with other modified support catalysts (Ru/CoMn₂O₄ and Ru/MnCo₂CO₃) under moderate reaction conditions (T = 120 °C, P_{air} = 24 bar and t = 10 h) with minor FFCA impurities [81]. In this study, it is concluded that catalyst supports structure plays vital role in catalytic activity. The high FDCA yield is due to Lewis and Brønsted active acid sites on catalytic surface which is confirmed by NH₃-TPD results (Figure 4). Variation in supports to CoMn₂O₄ and MnCo₂CO₃ adversely affects the catalytic activity and FDCA yield is decreased to 82.2% and 69.9%, respectively (Table 4).

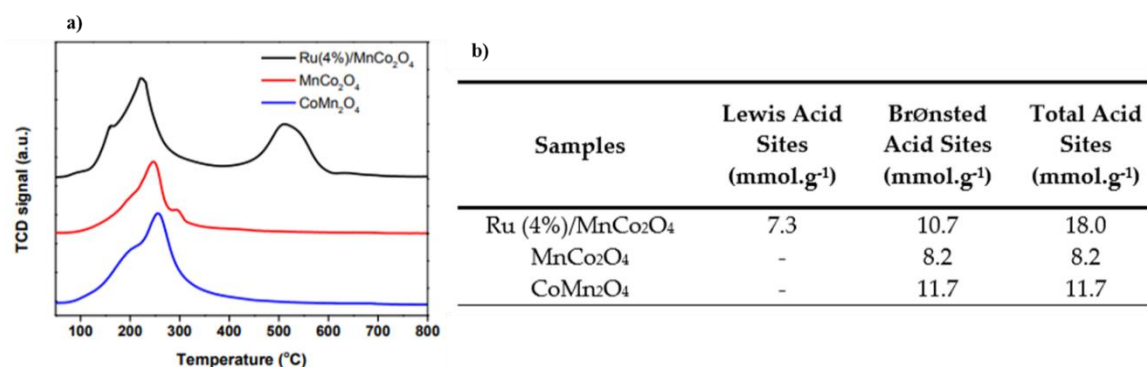


Figure 4. (a) NH₃-TPD and (b) summarized data obtained from NH₃-TPD for CoMn₂O₄, MnCo₂O₄ and Ru/MnCo₂O₄ catalyst (reproduced from [81] with permission from the Royal Society of Chemistry, copyright 2017).

Ru/HAP also shows good catalytic activity with 100% of HMF conversion and more than 99% of FDCA yield in base-free conditions [82]. This reaction is carried out in severe reaction conditions (T = 140 °C, P = 10 bar and t = 24 h) which is very challenging for practical applications. High catalytic performance of Ru/HAP catalyst is credited to formation of acidic-basic sites due to well dispersed Ru nanoparticles on HAP support. Christian and coworkers studied FDCA production via HMF oxidation over Ru catalyst supported on high surface area zirconia (ZrO₂) in a base-free environment [83]. High FDCA yield (97%) is achieved with 100% HMF conversion after 16 h reaction at similar severe reaction conditions (T = 120 °C and P = 10 bar). The catalytic tests in this investigation revealed that the small size of Ru particles due to utilization of high surface area ZrO₂ is crucial reason for better catalytic performance.

Rhodium (Rh) metal, in comparison with other noble metals (Ru, Pd, Au, and Pt), also has similar potential to act as catalytic active site in heterogeneous catalysis. However, this metal is not broadly explored by the researchers for catalytic oxidation of HMF to FDCA. This could be because of its high cost and less availability. Vuyyuru et al. have taken first step to use Rh to prepare a Rh/C catalyst for catalytic oxidation of HMF to FDCA [86]. The catalytic activity is compared for HMF oxidation reaction using different noble metals on carbon support at mild temperature (50 °C) and oxygen pressure (10 bar). The FDCA yield obtained in this work is 12.62%, which is comparatively low, with HMF conversion of 82%, after 4 h of reaction time over Rh/C catalysts. Ag-based catalysts were also studied for the aerobic oxidation of HMF to FDCA [87]. Inferior activities and selectivity to FDCA were shown with Ag-based catalysts, with HMFCAs as the primary product. In addition, leaching of Ag was also demonstrated to be another issue during catalysis. Therefore, rooms are available for the

improvement of catalytic performance of those noble-metal based catalysts in the aerobic oxidation of HMF into FDCA.

To sum up the overall results for the aerobic oxidation of HMF to FDCA over noble metal catalysts, a lot of progress has been achieved recently. Au catalysts are more effective catalysts in terms of stability and selectivity in comparison with Pt, Pd, Ru, and Rh based catalysts owing to a better ability in resistance to water and oxygen. However, deactivation of Au catalysts, and intermediates depositing on catalytic active sites are still observed for Au catalysts. Most of the studied noble metal catalysts use base additives to achieve high FDCA yield, to facilitate the oxidation of aldehyde part of HMF and keep the formed FDCA to dissolve into the solutions, in which the strong adsorption of products on the catalysts can be prevented. The aerial oxidation of HMF in base-free environment is a more green process, and more appropriate for sustainable chemistry. This entails a more research focus on base-free catalytic systems for the oxidation of HMF to FDCA. Applying an appropriate support and using an alloy strategy might make the catalysts show high activity and stability for the base-free oxidation of HMF into FDCA.

3. Non-Noble Metal Catalysts for FDCA Production

Noble metal catalysts are generally considered as active and stable in the field of catalysis, but due to their higher costs and less availability, it is of interest to design non-noble metal catalysts with high efficiency and excellent stability. Therefore, research shifted towards non-precious metal catalysts for aerobic oxidation of HMF to FDCA with prominent catalytic performance, and a reasonable progress has been achieved until now to get active and stable catalysts [88] (Table 5).

Table 5. Results of the oxidation of HMF to FDCA over non-noble metal catalysts.

Catalysts	Additive	Reaction Conditions			HMF Conv. (%)	FDCA Yield (%)	Ref.
		T (°C)	Oxidant P (bar)	Time (h)			
Fe-POP ^a	-	100	O ₂ , 10	10	100	85	[89]
MR-Co-Py ^b	CH ₃ CN	100	t-BuOOH	24	95.6	90.4	[90]
Li ₂ CoMn ₃ O ₈	CH ₃ COOH	150	Air, 55	8	100	80	[91]
Fe ₃ O ₄ -CoO _x	-	80	t-BuOOH	12	97.2	68.6	[92]
Ce _{0.5} Fe _{0.5} O ₂	[Bmim]Cl	140	O ₂ , 20	24	98.4	13.8	[93]
Ce _{0.5} Zr _{0.5} O ₂	[Bmim]Cl	140	O ₂ , 20	24	96.1	23.2	[93]
Ce _{0.5} Fe _{0.15} Zr _{0.35} O ₂	[Bmim]Cl	140	O ₂ , 20	24	99.9	44.2	[93]
Fe _{0.6} Zr _{0.4} O ₂	[Bmim]Cl	160	O ₂ , 20	24	99.7	60.6	[94]
MnO ₂	NaHCO ₃	100	O ₂ , 10	24	>99	91.0	[95]
MOF-Mn ₂ O ₃	NaHCO ₃	100	O ₂ , 14	24	100	99.5	[96]
MnO _x -CeO ₂	KHCO ₃	110	O ₂ , 20	15	98	91	[97]
MnCo ₂ O ₄	KHCO ₃	100	O ₂ , 20	24	99.5	70.9	[98]
Co ₃ O ₄ /Mn _x Co	Base free	140	O ₂ , 1	24	100	>99	[99]

^a POP = Porous organic polymer; ^b MR-Co-Py = Merrifield Resin supported Co(II)-*meso*-tetra(4-pyridyl)porphyrin.

Saha et al. prepared a thermally stable, robust structured iron catalyst (Fe/POP) by the integration of Fe³⁺ on the center of porphyrin ring supported on porous organic polymer (POP) to study the catalytic performance of aerobic oxidation of HMF to FDCA in aqueous medium [89]. This inexpensive metal catalyst can be reused without any significant loss of activity because the oxidation state of Fe remains intact after the reaction over this catalyst. As a result, complete HMF conversion was achieved with high FDCA yield (85%) at 100 °C and 10 bar O₂ pressure for 10 h reaction. The metal active site of Fe³⁺-POP catalyst plays a significant role and a plausible radical chain mechanism for HMF oxidation would involve thermal autoxidation of organic substrate (R-H) to peroxides (ROOH) which further lead to FDCA product through Fenton-type cleavage of RO-OH bond over Fe. Later on, a stable cobalt (II)-*meso*-tetra(4-pyridyl) porphyrin supported on Merrifield resin catalyst was developed (abbreviated as Merrifield Resin-Co-Py) by Gao et al. and studied the effect of various oxidants [90]. This catalyst showed excellent catalytic activity (FDCA yield = 90.4%, and HMF conversion = 95.6%) at 100 °C in

the presence of *tert*-butylhydroperoxide (*t*-BuOOH) as oxidant after 24 h reaction (Table 5). On the other hand, in the presence of O₂ as oxidant, no FDCA was detected after 24 h of reaction. Methyl nitrile (CH₃CN) was found to be the best solvent in this reaction system. Furthermore, Jain et al. introduced a low-cost Li₂CoMn₃O₈ (spinel-mixed metal oxide) catalyst prepared by gel pyrolysis method to study the catalytic oxidation of HMF to FDCA in the presence of sodium bromide and acetic acid [91]. Although a reasonable FDCA yield (80%) is obtained but use of high temperature (150 °C) along with acetic acid and sodium bromide additives are the main drawbacks for this route.

Similar to noble metal magnetic catalysts, Wang et al. prepared non-noble metal (nano-Fe₃O₄-CoO_x) catalysts with magnetic properties [92]. As demonstrated earlier, this catalyst can also be easily recovered using external magnet because of its magnetic properties. This magnetic catalyst showed 97.2% of HMF conversion with FDCA yield (68.6%) and reasonable reusability of catalyst with minor mass loss at 80 °C for 12 h reaction (Table 5). Experimental results in this study demonstrated that the first step of HMF oxidation to produce FFCA is initiated by Brønsted base, even without the presence of catalyst, whereas, the second step to produce FDCA from FFCA, requires the presence of catalysts. Similar conclusions were reached in another study of the catalytic oxidation of HMF to produce FFCA over a low cost Mn_{0.75}/Fe_{0.25} heterogeneous metal catalyst [100].

Ionic liquids or ionic fluids have also been studied as solvents for this reaction system together with low cost transition metal oxide catalysts [93,94]. Several combinations of iron oxide (Fe₂O₃) and zirconia (ZrO₂) have been used with different Fe to Zr ratios to develop a highly efficient catalyst. For this system, even though the attained FDCA yield is low, excellent conversion of HMF attracts researchers to dig more about its mechanism. The results illustrated that change in the reaction parameters and using different Fe to Zr proportions can hardly improve the catalytic activity (Table 5).

Manganese (Mn) based catalysts were also reported for the aerobic oxidation of HMF with base additives. MnO₂/NaHCO₃ system was reported by Hayashi et al. [95]. A FDCA yield of 91% with a complete HMF conversion could be obtained at 100 °C and 10 bar O₂ after 24 h of reaction. However, catalyst deactivation was observed in the third cycle of reuse runs, mainly owing to adsorbed humin species covering the active sites. Catalyst reactivation could be achieved by calcination at 300 °C in air. Hayashi et al. further studied the impact of the structure of MnO₂ crystal on the performance in the aerobic oxidation of HMF to FDCA through combined computational and experimental studies [101]. They demonstrated that reaction rates per surface area for the slowest step, FFCA oxidation to FDCA step, decrease in the order of β-MnO₂ > λ-MnO₂ > γ-MnO₂ ≈ α-MnO₂ > δ-MnO₂ > ε-MnO₂ on the basis of good agreements achieved between experimental results with the DFT calculations. β-MnO₂ exceeds that of the previously reported activated MnO₂. The successful synthesis of high-surface-area β-MnO₂ could significantly improve the catalytic activity for the aerobic oxidation of HMF to FDCA. Notably, a porous 2D Mn₂O₃ nanoflakes was prepared by a facile thermal treatment of a Mn-based metal-organic framework (MOF) precursor and applied for oxidation of HMF at 100 °C and 14 bar O₂ with NaHCO₃ [96]. A FDCA yield of 99.5% at complete conversion of HMF could be achieved after a reaction time of 24 h. However, a slight catalyst deactivation was observed during the recycle experiments.

Mixed/binary oxides have also been applied for the aerobic oxidation of HMF and showed enhanced catalytic performances as compared with their mono-oxide counterparts. Han et al prepared a mixed oxide MnO_x-CeO₂ (Mn/Ce = 6) catalyst by co-precipitation method, which afforded a high FDCA yield of 91% with a HMF conversion of 98% at 110 °C with KHCO₃ after 15 h reaction [97]. Structural analysis of mixed oxide catalyst revealed that the Mn⁴⁺ and Ce³⁺ on catalytic surface played the pivotal role as the active sites for HMF oxidation to FDCA. A mechanism involving the Mn⁴⁺ active center, the lattice oxygen transfer from CeO₂ to Mn oxide and the activation of O₂ on CeO₂ was proposed for the enhanced the performance. Mn-Co binary oxides catalysts with different Mn/Co molar ratios were also studied by Zhang et al. for catalytic oxidation of HMF to FDCA [98]. The MnCo₂O₄ catalyst with a Mn/Co molar ratios of 1/2, showed a HMF conversion of 99.5% and a FDCA yield of 70.9% at 100 °C and 10 bar O₂ with KHCO₃ for 24 h, which was significantly better than Mn₃O₄,

Co₃O₄ and Mn-Co binary oxides with other Mn/Co molar ratios. The enhanced catalytic activity was attributed to the presence of Mn³⁺ ions and the high oxygen mobility and reducibility.

The aerobic base-free oxidation of HMF to FDCA over non-precious metal catalysts has been limited reported. The use of organic solvent, organic peroxide and base additives may promote the product yield but undoubtedly hamper the green footprint of renewable FEDA production. It is still rather difficult to use non-noble metal based catalysts for the aerobic oxidation of HMF to FDCA in water and without base additives. Recently, Gao et al. prepared a Mn-Co mixed oxide catalyst (Co₃O₄/Mn_xCo) with Co₃O₄ nanoparticles well-dispersed on amorphous Mn-Co-O solid solutions by co-precipitation method [99]. They claimed that a FDCA yield of >99% could be obtained with Co₃O₄/Mn_{0.2}Co where the Mn/Co ratio was of 0.2, at 1 bar O₂ and 140 °C after 24 h without base additives. The high content of both Lewis (Mn⁴⁺) and Brønsted (Co–O–H⁺) acid sites on the surface, leading to an excellent ability of HMF adsorption and COOH group formation, as well as the enhanced oxygen mobility. This catalyst was shown stable after a minor deactivation (≤8%) during six recycling uses and its activity could be entirely regenerated by calcination in air.

According to the results of the aerobic oxidation of HMF to FDCA over non-noble metal based catalysts (Fe-, Co-, and Mn-based), an inferior catalytic selectivity to FDCA is normally shown as compared to noble metal catalysts. The activation of O₂ is not very efficient (especially Fe- and Co-based) and a strong oxidant (e.g., *t*-BuOOH) is more normally required to obtain a good selectivity of FDCA. Especially, base additives and organic solvent are often required to improve the FDCA yield. The stability of non-noble metal based catalyst suffers from more issues, i.e., metal leaching (especially Ni- and Cu-based), change of the active phase, and coverage of active species. Still, owing to the advance in the cost, it is promising to further explore non-precious transition-metal catalysts considering the lower catalyst cost for the upcoming practical production of FDCA. Therefore, further effort should be continuously devoted to develop new approaches for designing efficient non-precious transition-metal catalysts for the aerobic oxidation of HMF to FDCA.

4. Conclusions and Perspectives

The catalytic aerobic oxidation of biomass-derived HMF to FDCA is currently a hot topic, especially since FDCA exhibits the potential to replace petrochemical-derived terephthalic acid, one of the most widely used monomers in polymers, for the production of a series of biopolymers. According to the recent results of the aerobic oxidation of HMF to FDCA over supported metal catalysts, noble-metal catalysts are the most studied. Much progress and numerous breakthroughs have already been made in catalyst design and understanding the reaction mechanism. Although the application of inexpensive transition-metal catalysts might offer promising prospects in the practical synthesis of FDCA, the main issue of the non-noble metal-based catalyst is the inferior selectivity for FDCA compared to the noble-metal analogues, based on currently reported methods. Additional research efforts should be devoted to develop new methods based on non-noble transition-metal catalysts that can improve the selectivity of FDCA, especially with O₂ as the oxidant and without using additional base. The performance of the catalyst and the reaction pathway are highly dependent on the properties of the catalyst (i.e., the active phase, support, particle size) and reaction conditions (i.e., oxygen pressure, oxygen flow rate, pH, and temperature). Among the noble metal-based catalysts, Au-based catalysts appear to show a better performance in catalyst selectivity and stability for the aerobic oxidation of HMF into FDCA in water, compared to the Pt-, Pd-, Ru-, and Rh-based catalysts, owing to the better resistance to water and O₂. Nevertheless, deactivation of the Au-based catalysts by the deposition of the byproducts or intermediates on its active sites is also observed, as mentioned in some examples. For further improvement of the Au-based catalyst, a bimetallic alloy approach, achieved by alloying of a second metal with Au, has been applied and shown to be effective, with a higher catalytic activity and improved stability as compared to the monometallic counterparts. Although many bi-functional combinations have shown promising outcomes with rate enhancement or a synergistic effect. More details into how such effect of different function sites comes from metals or other sites with an optimal

site-balance, have been limitedly studied. Better insight of the reaction mechanisms involved needs to be provided on atomic levels for the oxidation of HMF into FDCA.

Normally, excess base is used to promote the oxidation of HMF, which can not only facilitate the reaction, but also transform the formed FDCA into a salt form dissolved in aqueous solution. Otherwise, the strong adsorption of the carboxylic acids on the catalyst can hinder the further process of this reaction. The use of excess base can however also lead to a more expensive process, which is also less green. Therefore, it is necessary to develop a base-free oxidation system, which is more cost-effective and environmentally benign approach, appreciated in sustainable chemistry. Selecting an appropriate support with basic sites for the catalysts has shown advantages in catalytic activity and stability for the base-free oxidation of HMF into FDCA in recent examples. However, catalyst deactivation owing to a loss in basic sites has been observed with the support during reactions, and the stability of the catalyst is found to be a challenge for the catalyst. More effort needs to be put into finding out how to stabilize the required functional sites on the catalyst, and advanced strategies of catalyst design for preparing specific structures, i.e., single-atom metal, core-shell, sub-cluster segregated, multi-shell and random homogeneous alloys, etc., deserve more thoroughly exploration in research.

Most reported studies with high FDCA yields in the aerobic oxidation of HMF, have been conducted in dilute HMF solutions (0.5–2.1 wt%), which is unreal for the practical production of FDCA on an industrial scale. The limitation is attributed to the highly reactive functional groups in HMF, which can lead to the formation of undesired solid byproducts, namely humins, via complex side reactions (i.e., condensation and polymerization). Many fewer examples of concentrated HMF substrates are studied in the oxidation of HMF to FDCA. Recently, an approach for stabilizing the active formyl group of HMF by the acetalization with 1,3-propanediol was reported, which enables production of a high yield of FDCA and low humin formation, even in solutions of up to 20 wt% HMF acetal, by aerobic oxidation in the presence of a base additive [38]. In addition, extremely low concentration of HMF, together with their short-term reaction time often applied in reported cases, may underestimate other issues, particularly catalyst stability. Catalyst deactivation might not be well recognized in the liquid phase with a higher concentration of HMF (polar, aqueous and even corrosive). Thus, research efforts are still needed to conduct the reactions under a more practical concentration of HMF, and further understand the deeper fundamentals of catalyst stability challenges, in order to develop innovative and creative approaches.

The reaction mechanisms involved in the aerobic oxidation of HMF were revealed with some metal-based catalysts, mainly by applying isotope labeling and mass spectrometric techniques. Still, more efforts need to be devoted to the development of modern in-situ characterization technologies, to provide deep insights into the intrinsic kinetics and mechanisms. In addition, the state-of-the-art *operando* characterization methods combined with various spectroscopy techniques are also necessary for understanding the deep fundamentals of the nature of the intrinsic active sites for each elemental step in HMF oxidation, which might dynamically evaluate during catalysis [102]. The adequate understanding of the reaction mechanism will elucidate a more detailed understanding of catalytic chemistry. The deep insights on the active site can greatly benefit the rational design of catalysts, even with the use of the non-noble metals to prepare more efficient and stable catalysts for the oxidation of HMF to FDCA.

Although many significant achievements have been made for the aerobic oxidation of HMF to FDCA over metal-based heterogeneous catalysts, further improvements are still required for scaling up to an industrially large-scale production of FDCA. The mass balances for the aerobic oxidation of HMF to FDCA based on laboratory data need to be accurate and correct. The mass balance for the oxidation of HMF was not always mentioned or even not fully closed in many cases. Those unknown parameters might result in a significant amount of economic loss during scaling up processes if not properly done. Current approaches for the pioneering processes for the production of FDCA from HMF are technically feasible but not economically viable, mainly owing to the high price of HMF and its limited availability. Development of energetically and economically viable processes is a long-term task which requires

extensive time, efforts and normally involves interdisciplinary knowledge of process engineering, chemistry, material science, etc. Only with a full grasp of the knowledge and reorganization of the fundamental details and catalytic challenges, we may develop an economically feasible approach for realizing industrially large-scale production of FDCA in the near future, which will alleviate our society's dependence on the traditional fossil resources.

Author Contributions: Conceptualization, S.H. and W.L.; validation, W.L.; formal analysis, L.L. and W.L.; investigation, S.H., L.L. and W.L.; resources A.W. and W.L.; writing—original draft preparation, S.H.; writing—review and editing, L.L.; supervision, A.W. and W.L. All authors have read and agreed to the published version of the manuscript.

Funding: This research was funded by the National Key Projects for Fundamental Research and Development of China (2018YFB1501602) and the National Natural Science Foundation of China (21703238, 21690084).

Acknowledgments: The authors acknowledge the National Key Projects for Fundamental Research and Development of China (2018YFB1501602), the National Natural Science Foundation of China (21703238, 21690084) and the CAS-TWAS President's Fellowship Program between Chinese Academy of Sciences (CAS) and The World Academy of Sciences (TWAS) for financial support.

Conflicts of Interest: The authors declare no conflict of interest.

References

1. Bozell, J.J. Connecting Biomass and Petroleum Processing with a Chemical Bridge. *Science* **2010**, *329*, 522–523. [[CrossRef](#)] [[PubMed](#)]
2. Corma, A.; Iborra, S.; Velty, A. Chemical routes for the transformation of biomass into chemicals. *Chem. Rev.* **2007**, *107*, 2411–2502. [[CrossRef](#)] [[PubMed](#)]
3. Gallezot, P. Conversion of biomass to selected chemical products. *Chem. Soc. Rev.* **2012**, *41*, 1538–1558. [[CrossRef](#)] [[PubMed](#)]
4. H. Clark, J.; El Deswarte, F.; J. Farmer, T. The integration of green chemistry into future biorefineries. *Biofuels Bioprod. Biorefin.* **2009**, *3*, 72–90. [[CrossRef](#)]
5. Roy Goswami, S.; Dumont, M.-J.; Raghavan, V. Starch to value added biochemicals. *Starch Stärke* **2016**, *68*, 274–286. [[CrossRef](#)]
6. Morais, A.R.; da Costa Lopes, A.M.; Bogel-Lukasik, R. Carbon dioxide in biomass processing: Contributions to the green biorefinery concept. *Chem. Rev.* **2014**, *115*, 3–27. [[CrossRef](#)]
7. Van Putten, R.-J.; van der Waal, J.C.; de Jong, E.; Rasrendra, C.B.; Heeres, H.J.; de Vries, J.G. Hydroxymethylfurfural, A Versatile Platform Chemical Made from Renewable Resources. *Chem. Rev.* **2013**, *113*, 1499–1597. [[CrossRef](#)]
8. Fukuoka, A.; Dhepe, P.L. Catalytic Conversion of Cellulose into Sugar Alcohols. *Angew. Chem. Int. Ed.* **2006**, *45*, 5161–5163. [[CrossRef](#)]
9. Deng, W.; Zhang, Q.; Wang, Y. Polyoxometalates as efficient catalysts for transformations of cellulose into platform chemicals. *Dalton Trans.* **2012**, *41*, 9817–9831. [[CrossRef](#)]
10. Rinaldi, R.; Schüth, F. Acid Hydrolysis of Cellulose as the Entry Point into Biorefinery Schemes. *ChemSusChem* **2009**, *2*, 1096–1107. [[CrossRef](#)]
11. Pal, P.; Saravanamurugan, S. Recent Advances in the Development of 5-Hydroxymethylfurfural Oxidation with Base (Nonprecious)-Metal-Containing Catalysts. *ChemSusChem* **2019**, *12*, 145–163. [[CrossRef](#)]
12. Werpy, T.; Petersen, G. *Top Value Added Chemicals from Biomass: Volume I—Results of Screening for Potential Candidates from Sugars and Synthesis Gas*; National Renewable Energy Lab.: Golden, CO, USA, 2004.
13. Haworth, W.N.; Jones, W.G.M.; Wiggins, L.F. 1. The conversion of sucrose into furan compounds. Part II. Some 2: 5-disubstituted tetrahydrofurans and their products of ring scission. *J. Chem. Soc.* **1945**, *10*, 1–4. [[CrossRef](#)]
14. Chen, M.Y.; Ike, M.; Fujita, M. Acute toxicity, mutagenicity, and estrogenicity of bisphenol-A and other bisphenols. *Environ. Toxicol. Int. J.* **2002**, *17*, 80–86. [[CrossRef](#)] [[PubMed](#)]
15. Swan, S.H. Environmental phthalate exposure in relation to reproductive outcomes and other health endpoints in humans. *Environ. Res.* **2008**, *108*, 177–184. [[CrossRef](#)] [[PubMed](#)]
16. Ravindranath, K.; Mashelkar, R.A. Polyethylene terephthalate-I. Chemistry, thermodynamics and transport properties. *Chem. Eng. Sci.* **1986**, *41*, 2197–2214. [[CrossRef](#)]

17. Chen, G.; van Straalen, N.M.; Roelofs, D. The ecotoxicogenomic assessment of soil toxicity associated with the production chain of 2,5-furandicarboxylic acid (FDCA), a candidate bio-based green chemical building block. *Green Chem.* **2016**, *18*, 4420–4431. [[CrossRef](#)]
18. Lancefield, C.S.; Teunissen, L.W.; Weckhuysen, B.M.; Bruijninx, P.C. Iridium-catalysed primary alcohol oxidation and hydrogen shuttling for the depolymerisation of lignin. *Green Chem.* **2018**, *20*, 3214–3221. [[CrossRef](#)]
19. De Jong, E.; Dam, M.; Sipos, L.; Gruter, G.-J. Furandicarboxylic acid (FDCA), a versatile building block for a very interesting class of polyesters. In *Biobased Monomers, Polymers, and Materials*; ACS Symposium Series; American Chemical Society: Washington, DC, USA, 2012; pp. 1–13.
20. Pan, T.; Deng, J.; Xu, Q.; Zuo, Y.; Guo, Q.X.; Fu, Y. Catalytic Conversion of Furfural into a 2,5-Furandicarboxylic Acid-Based Polyester with Total Carbon Utilization. *ChemSusChem* **2013**, *6*, 47–50. [[CrossRef](#)]
21. Ball, G.L.; McLellan, C.J.; Bhat, V.S. Toxicological review and oral risk assessment of terephthalic acid (TPA) and its esters: A category approach. *Crit. Rev. Toxicol.* **2012**, *42*, 28–67. [[CrossRef](#)]
22. Eerhart, A.J.J.E.; Faaij, A.P.C.; Patel, M.K. Replacing fossil based PET with biobased PEF; process analysis, energy and GHG balance. *Energy Environ. Sci.* **2012**, *5*, 6407–6422. [[CrossRef](#)]
23. Fittig, R.; Heinzelmann, H. Production of 2,5-furandicarboxylic acid by the reaction of fuming hydrobromic acid with mucic acid under pressure. *Chem. Ber.* **1876**, *9*, 1198.
24. Rose, M.; Weber, D.; Lotsch, B.V.; Kremer, R.K.; Goddard, R.; Palkovits, R. Biogenic metal–organic frameworks: 2,5-Furandicarboxylic acid as versatile building block. *Microporous Mesoporous Mater.* **2013**, *181*, 217–221. [[CrossRef](#)]
25. Chadderdon, D.J.; Xin, L.; Qi, J.; Qiu, Y.; Krishna, P.; More, K.L.; Li, W. Electrocatalytic oxidation of 5-hydroxymethylfurfural to 2,5-furandicarboxylic acid on supported Au and Pd bimetallic nanoparticles. *Green Chem.* **2014**, *16*, 3778–3786. [[CrossRef](#)]
26. Wang, K.F.; Liu, C.L.; Sui, K.Y.; Guo, C.; Liu, C.Z. Efficient Catalytic Oxidation of 5-Hydroxymethylfurfural to 2,5-Furandicarboxylic Acid by Magnetic Laccase Catalyst. *ChemBioChem* **2018**, *19*, 654–659. [[CrossRef](#)] [[PubMed](#)]
27. Ban, H.; Pan, T.; Cheng, Y.; Wang, L.; Li, X. Solubilities of 2,5-Furandicarboxylic Acid in Binary Acetic Acid + Water, Methanol + Water, and Ethanol + Water Solvent Mixtures. *J. Chem. Eng. Data* **2018**, *63*, 1987–1993. [[CrossRef](#)]
28. Sajid, M.; Zhao, X.; Liu, D. Production of 2,5-furandicarboxylic acid (FDCA) from 5-hydroxymethylfurfural (HMF): Recent progress focusing on the chemical-catalytic routes. *Green Chem.* **2018**, *20*, 5427–5453. [[CrossRef](#)]
29. Xuan, Y.; He, R.; Han, B.; Wu, T.; Wu, Y. Catalytic Conversion of Cellulose into 5-Hydroxymethylfurfural Using [PSMIM] HSO₄ and ZnSO₄·7H₂O Co-catalyst in Biphasic System. *Waste Biomass Valoriz.* **2018**, *9*, 401–408. [[CrossRef](#)]
30. Dijkman, W.P.; Groothuis, D.E.; Fraaije, M.W. Enzyme-Catalyzed Oxidation of 5-Hydroxymethylfurfural to Furan-2,5-dicarboxylic Acid. *Angew. Chem. Int. Ed.* **2014**, *53*, 6515–6518. [[CrossRef](#)]
31. Chen, C.T.; Nguyen, C.V.; Wang, Z.Y.; Bando, Y.; Yamauchi, Y.; Bazziz, M.T.S.; Fatehmulla, A.; Farooq, W.A.; Yoshikawa, T.; Masuda, T. Hydrogen Peroxide Assisted Selective Oxidation of 5-Hydroxymethylfurfural in Water under Mild Conditions. *ChemCatChem* **2018**, *10*, 361–365. [[CrossRef](#)]
32. Nam, D.-H.; Taitt, B.J.; Choi, K.-S. Copper-Based Catalytic Anodes To Produce 2,5-Furandicarboxylic Acid, a Biomass-Derived Alternative to Terephthalic Acid. *ACS Catal.* **2018**, *8*, 1197–1206. [[CrossRef](#)]
33. Xu, S.; Zhou, P.; Zhang, Z.; Yang, C.; Zhang, B.; Deng, K.; Bottle, S.; Zhu, H. Selective Oxidation of 5-Hydroxymethylfurfural to 2,5-Furandicarboxylic Acid Using O₂ and a Photocatalyst of Co-thioporphyrazine Bonded to g-C₃N₄. *J. Am. Chem. Soc.* **2017**, *139*, 14775–14782. [[CrossRef](#)] [[PubMed](#)]
34. Hutchings, G.J. Vapor phase hydrochlorination of acetylene: Correlation of catalytic activity of supported metal chloride catalysts. *J. Catal.* **1985**, *96*, 292–295. [[CrossRef](#)]
35. Masatake, H.; Tetsuhiko, K.; Hiroshi, S.; Nobumasa, Y. Novel Gold Catalysts for the Oxidation of Carbon Monoxide at a Temperature far Below 0 °C. *Chem. Lett.* **1987**, *16*, 405–408.
36. Casanova, O.; Iborra, S.; Corma, A. Biomass into Chemicals: Aerobic Oxidation of 5-Hydroxymethyl-2-furfural into 2,5-Furandicarboxylic Acid with Gold Nanoparticle Catalysts. *ChemSusChem* **2009**, *2*, 1138–1144. [[CrossRef](#)] [[PubMed](#)]

37. Lolli, A.; Amadori, R.; Lucarelli, C.; Cutrufello, M.G.; Rombi, E.; Cavani, F.; Albonetti, S. Hard-template preparation of Au/CeO₂ mesostructured catalysts and their activity for the selective oxidation of 5-hydroxymethylfurfural to 2,5-furandicarboxylic acid. *Microporous Mesoporous Mater.* **2016**, *226*, 466–475. [[CrossRef](#)]
38. Kim, M.; Su, Y.; Fukuoka, A.; Hensen, E.J.M.; Nakajima, K. Aerobic Oxidation of 5-(Hydroxymethyl)furfural Cyclic Acetal Enables Selective Furan-2,5-dicarboxylic Acid Formation with CeO₂-Supported Gold Catalyst. *Angew. Chem. Int. Ed.* **2018**, *57*, 8235–8239. [[CrossRef](#)]
39. Gorbanev, Y.Y.; Klitgaard, S.K.; Woodley, J.M.; Christensen, C.H.; Riisager, A. Gold-Catalyzed Aerobic Oxidation of 5-Hydroxymethylfurfural in Water at Ambient Temperature. *ChemSusChem* **2009**, *2*, 672–675. [[CrossRef](#)]
40. Cai, J.; Ma, H.; Zhang, J.; Song, Q.; Du, Z.; Huang, Y.; Xu, J. Gold Nanoclusters Confined in a Supercage of Y Zeolite for Aerobic Oxidation of HMF under Mild Conditions. *Chem. Eur. J.* **2013**, *19*, 14215–14223. [[CrossRef](#)]
41. Pasini, T.; Piccinini, M.; Blosi, M.; Bonelli, R.; Albonetti, S.; Dimitratos, N.; Lopez-Sanchez, J.A.; Sankar, M.; He, Q.; Kiely, C.J.; et al. Selective oxidation of 5-hydroxymethyl-2-furfural using supported gold–copper nanoparticles. *Green Chem.* **2011**, *13*, 2091–2099. [[CrossRef](#)]
42. Villa, A.; Schiavoni, M.; Campisi, S.; Veith, G.M.; Prati, L. Pd-modified Au on Carbon as an Effective and Durable Catalyst for the Direct Oxidation of HMF to 2,5-Furandicarboxylic Acid. *ChemSusChem* **2013**, *6*, 609–612. [[CrossRef](#)]
43. Gupta, N.K.; Nishimura, S.; Takagaki, A.; Ebitani, K. Hydrotalcite-supported gold-nanoparticle-catalyzed highly efficient base-free aqueous oxidation of 5-hydroxymethylfurfural into 2,5-furandicarboxylic acid under atmospheric oxygen pressure. *Green Chem.* **2011**, *13*, 824–827. [[CrossRef](#)]
44. Gao, T.; Gao, T.; Fang, W.; Cao, Q. Base-free aerobic oxidation of 5-hydroxymethylfurfural to 2,5-furandicarboxylic acid in water by hydrotalcite-activated carbon composite supported gold catalyst. *Mol. Catal.* **2017**, *439*, 171–179. [[CrossRef](#)]
45. Wan, X.; Zhou, C.; Chen, J.; Deng, W.; Zhang, Q.; Yang, Y.; Wang, Y. Base-Free Aerobic Oxidation of 5-Hydroxymethyl-furfural to 2,5-Furandicarboxylic Acid in Water Catalyzed by Functionalized Carbon Nanotube-Supported Au–Pd Alloy Nanoparticles. *ACS Catal.* **2014**, *4*, 2175–2185. [[CrossRef](#)]
46. Bonincontro, D.; Lolli, A.; Villa, A.; Prati, L.; Dimitratos, N.; Veith, G.M.; Chinchilla, L.E.; Botton, G.A.; Cavani, F.; Albonetti, S. AuPd-nNiO as an effective catalyst for the base-free oxidation of HMF under mild reaction conditions. *Green Chem.* **2019**, *21*, 4090–4099. [[CrossRef](#)]
47. Gao, Z.; Xie, R.; Fan, G.; Yang, L.; Li, F. Highly Efficient and Stable Bimetallic AuPd over La-Doped Ca–Mg–Al Layered Double Hydroxide for Base-Free Aerobic Oxidation of 5-Hydroxymethylfurfural in Water. *ACS Sustain. Chem. Eng.* **2017**, *5*, 5852–5861. [[CrossRef](#)]
48. Davis, S.E.; Zope, B.N.; Davis, R.J. On the mechanism of selective oxidation of 5-hydroxymethylfurfural to 2,5-furandicarboxylic acid over supported Pt and Au catalysts. *Green Chem.* **2012**, *14*, 143–147. [[CrossRef](#)]
49. Davis, S.E.; Benavidez, A.D.; Gosselink, R.W.; Bitter, J.H.; de Jong, K.P.; Dartye, A.K.; Davis, R.J. Kinetics and mechanism of 5-hydroxymethylfurfural oxidation and their implications for catalyst development. *J. Mol. Catal. A* **2014**, *388*, 123–132. [[CrossRef](#)]
50. Zope, B.N.; Hibbitts, D.D.; Neurock, M.; Davis, R.J. Reactivity of the gold/water interface during selective oxidation catalysis. *Science* **2010**, *330*, 74–78. [[CrossRef](#)]
51. Zope, B.N.; Davis, S.E.; Davis, R.J. Influence of reaction conditions on diacid formation during Au-catalyzed oxidation of glycerol and hydroxymethylfurfural. *Top. Catal.* **2012**, *55*, 24–32. [[CrossRef](#)]
52. Verdeguer, P.; Merat, N.; Gaset, A. Oxydation catalytique du HMF en acide 2,5-furane dicarboxylique. *J. Mol. Catal.* **1993**, *85*, 327–344. [[CrossRef](#)]
53. Rass, H.A.; Essayem, N.; Besson, M. Selective aqueous phase oxidation of 5-hydroxymethylfurfural to 2,5-furandicarboxylic acid over Pt/C catalysts: Influence of the base and effect of bismuth promotion. *Green Chem.* **2013**, *15*, 2240–2251. [[CrossRef](#)]
54. Ait Rass, H.; Essayem, N.; Besson, M. Selective Aerobic Oxidation of 5-HMF into 2,5-Furandicarboxylic Acid with Pt Catalysts Supported on TiO₂- and ZrO₂-Based Supports. *ChemSusChem* **2015**, *8*, 1206–1217. [[CrossRef](#)] [[PubMed](#)]
55. Sahu, R.; Dhepe, P.L. Synthesis of 2,5-furandicarboxylic acid by the aerobic oxidation of 5-hydroxymethyl furfural over supported metal catalysts. *React. Kinet. Mech. Catal.* **2014**, *112*, 173–187. [[CrossRef](#)]

56. Miao, Z.; Wu, T.; Li, J.; Yi, T.; Zhang, Y.; Yang, X. Aerobic oxidation of 5-hydroxymethylfurfural (HMF) effectively catalyzed by a $\text{Ce}_{0.8}\text{Bi}_{0.2}\text{O}_{2-\delta}$ supported Pt catalyst at room temperature. *RSC Adv.* **2015**, *5*, 19823–19829. [[CrossRef](#)]
57. Niu, W.; Wang, D.; Yang, G.; Sun, J.; Wu, M.; Yoneyama, Y.; Tsubaki, N. Pt Nanoparticles Loaded on Reduced Graphene Oxide as an Effective Catalyst for the Direct Oxidation of 5-Hydroxymethylfurfural (HMF) to Produce 2,5-Furandicarboxylic Acid (FDCA) under Mild Conditions. *Bull. Chem. Soc. Jpn.* **2014**, *87*, 1124–1129. [[CrossRef](#)]
58. Zhang, Y.; Xue, Z.; Wang, J.; Zhao, X.; Deng, Y.; Zhao, W.; Mu, T. Controlled deposition of Pt nanoparticles on Fe_3O_4 @carbon microspheres for efficient oxidation of 5-hydroxymethylfurfural. *RSC Adv.* **2016**, *6*, 51229–51237. [[CrossRef](#)]
59. Vinke, P.; van Dam, H.E.; van Bekkum, H. Platinum Catalyzed Oxidation of 5-Hydroxymethylfurfural. In *Studies in Surface Science and Catalysis*; Centi, G., Trifiro, F., Eds.; Elsevier: Amsterdam, The Netherlands, 1990; Volume 55, pp. 147–158.
60. Chen, H.; Shen, J.; Chen, K.; Qin, Y.; Lu, X.; Ouyang, P.; Fu, J. Atomic layer deposition of Pt nanoparticles on low surface area zirconium oxide for the efficient base-free oxidation of 5-hydroxymethylfurfural to 2,5-furandicarboxylic acid. *Appl. Catal. A Gen.* **2018**, *555*, 98–107. [[CrossRef](#)]
61. Han, X.; Geng, L.; Guo, Y.; Jia, R.; Liu, X.; Zhang, Y.; Wang, Y. Base-free aerobic oxidation of 5-hydroxymethylfurfural to 2,5-furandicarboxylic acid over a Pt/C–O–Mg catalyst. *Green Chem.* **2016**, *18*, 1597–1604. [[CrossRef](#)]
62. Han, X.; Li, C.; Guo, Y.; Liu, X.; Zhang, Y.; Wang, Y. N-doped carbon supported Pt catalyst for base-free oxidation of 5-hydroxymethylfurfural to 2,5-furandicarboxylic acid. *Appl. Catal. A Gen.* **2016**, *526*, 1–8. [[CrossRef](#)]
63. Shen, J.; Chen, H.; Chen, K.; Qin, Y.; Lu, X.; Ouyang, P.; Fu, J. Atomic Layer Deposition of a Pt-Skin Catalyst for Base-Free Aerobic Oxidation of 5-Hydroxymethylfurfural to 2,5-Furandicarboxylic Acid. *Ind. Eng. Chem. Res.* **2018**, *57*, 2811–2818. [[CrossRef](#)]
64. Siankevich, S.; Savoglidis, G.; Fei, Z.; Laurenczy, G.; Alexander, D.T.; Yan, N.; Dyson, P.J. A novel platinum nanocatalyst for the oxidation of 5-Hydroxymethylfurfural into 2,5-Furandicarboxylic acid under mild conditions. *J. Catal.* **2014**, *315*, 67–74. [[CrossRef](#)]
65. Siankevich, S.; Mozzettini, S.; Bobbink, F.; Ding, S.; Fei, Z.; Yan, N.; Dyson, P.J. Influence of the Anion on the Oxidation of 5-Hydroxymethylfurfural by Using Ionic-Polymer-Supported Platinum Nanoparticle Catalysts. *ChemPlusChem* **2018**, *83*, 19–23. [[CrossRef](#)]
66. Davis, S.E.; Houk, L.R.; Tamargo, E.C.; Datye, A.K.; Davis, R.J. Oxidation of 5-hydroxymethylfurfural over supported Pt, Pd and Au catalysts. *Catal. Today* **2011**, *160*, 55–60. [[CrossRef](#)]
67. Siyo, B.; Schneider, M.; Radnik, J.; Pohl, M.-M.; Langer, P.; Steinfeldt, N. Influence of support on the aerobic oxidation of HMF into FDCA over preformed Pd nanoparticle based materials. *Appl. Catal. A Gen.* **2014**, *478*, 107–116. [[CrossRef](#)]
68. Siyo, B.; Schneider, M.; Pohl, M.-M.; Langer, P.; Steinfeldt, N. Synthesis, characterization, and application of PVP-Pd NP in the aerobic oxidation of 5-hydroxymethylfurfural (hmf). *Catal. Lett.* **2014**, *144*, 498–506. [[CrossRef](#)]
69. Rathod, P.V.; Jadhav, V.H. Efficient Method for Synthesis of 2,5-Furandicarboxylic Acid from 5-Hydroxymethylfurfural and Fructose Using Pd/CC Catalyst under Aqueous Conditions. *ACS Sustain. Chem. Eng.* **2018**, *6*, 5766–5771. [[CrossRef](#)]
70. Zhang, Z.; Zhen, J.; Liu, B.; Lv, K.; Deng, K. Selective aerobic oxidation of the biomass-derived precursor 5-hydroxymethylfurfural to 2,5-furandicarboxylic acid under mild conditions over a magnetic palladium nanocatalyst. *Green Chem.* **2015**, *17*, 1308–1317. [[CrossRef](#)]
71. Mei, N.; Liu, B.; Zheng, J.; Lv, K.; Tang, D.; Zhang, Z. A novel magnetic palladium catalyst for the mild aerobic oxidation of 5-hydroxymethylfurfural into 2,5-furandicarboxylic acid in water. *Catal. Sci. Technol.* **2015**, *5*, 3194–3202. [[CrossRef](#)]
72. Liu, B.; Ren, Y.; Zhang, Z. Aerobic oxidation of 5-hydroxymethylfurfural into 2,5-furandicarboxylic acid in water under mild conditions. *Green Chem.* **2015**, *17*, 1610–1617. [[CrossRef](#)]
73. Lolli, A.; Albonetti, S.; Utili, L.; Amadori, R.; Ospitali, F.; Lucarelli, C.; Cavani, F. Insights into the reaction mechanism for 5-hydroxymethylfurfural oxidation to FDCA on bimetallic Pd–Au nanoparticles. *Appl. Catal. A Gen.* **2015**, *504*, 408–419. [[CrossRef](#)]

74. Xia, H.; An, J.; Hong, M.; Xu, S.; Zhang, L.; Zuo, S. Aerobic oxidation of 5-hydroxymethylfurfural to 2,5-difurancarboxylic acid over Pd-Au nanoparticles supported on Mg-Al hydrotalcite. *Catal. Today* **2019**, *319*, 113–120. [[CrossRef](#)]
75. Gupta, K.; Rai, R.K.; Singh, S.K. Catalytic aerial oxidation of 5-hydroxymethyl-2-furfural to furan-2,5-dicarboxylic acid over Ni-Pd nanoparticles supported on Mg(OH)₂ nanoflakes for the synthesis of furan diesters. *Inorg. Chem. Front.* **2017**, *4*, 871–880. [[CrossRef](#)]
76. Wang, Y.; Yu, K.; Lei, D.; Si, W.; Feng, Y.; Lou, L.-L.; Liu, S. Basicity-Tuned Hydrotalcite-Supported Pd Catalysts for Aerobic Oxidation of 5-Hydroxymethyl-2-furfural under Mild Conditions. *ACS Sustain. Chem. Eng.* **2016**, *4*, 4752–4761. [[CrossRef](#)]
77. Zakrzewska, M.E.; Bogel-Lukasik, E.; Bogel-Lukasik, R. Ionic Liquid-Mediated Formation of 5-Hydroxymethylfurfural—A Promising Biomass-Derived Building Block. *Chem. Rev.* **2011**, *111*, 397–417. [[CrossRef](#)]
78. Yi, G.; Teong, S.P.; Zhang, Y. Base-free conversion of 5-hydroxymethylfurfural to 2,5-furandicarboxylic acid over a Ru/C catalyst. *Green Chem.* **2016**, *18*, 979–983. [[CrossRef](#)]
79. Kerdi, F.; Ait Rass, H.; Pinel, C.; Besson, M.; Peru, G.; Leger, B.; Rio, S.; Monflier, E.; Ponchel, A. Evaluation of surface properties and pore structure of carbon on the activity of supported Ru catalysts in the aqueous-phase aerobic oxidation of HMF to FDCA. *Appl. Catal. A Gen.* **2015**, *506*, 206–219. [[CrossRef](#)]
80. Ståhlberg, T.; Eyjólfssdóttir, E.; Gorbanev, Y.Y.; Sádaba, I.; Riisager, A. Aerobic oxidation of 5-(hydroxymethyl) furfural in ionic liquids with solid ruthenium hydroxide catalysts. *Catal. Lett.* **2012**, *142*, 1089–1097. [[CrossRef](#)]
81. Mishra, D.K.; Lee, H.J.; Kim, J.; Lee, H.-S.; Cho, J.K.; Suh, Y.-W.; Yi, Y.; Kim, Y.J. MnCo₂O₄ spinel supported ruthenium catalyst for air-oxidation of HMF to FDCA under aqueous phase and base-free conditions. *Green Chem.* **2017**, *19*, 1619–1623. [[CrossRef](#)]
82. Gao, T.; Yin, Y.; Fang, W.; Cao, Q. Highly dispersed ruthenium nanoparticles on hydroxyapatite as selective and reusable catalyst for aerobic oxidation of 5-hydroxymethylfurfural to 2,5-furandicarboxylic acid under base-free conditions. *Mol. Catal.* **2018**, *450*, 55–64. [[CrossRef](#)]
83. Pichler, C.M.; Al-Shaal, M.G.; Gu, D.; Joshi, H.; Ciptonugroho, W.; Schüth, F. Ruthenium Supported on High-Surface-Area Zirconia as an Efficient Catalyst for the Base-Free Oxidation of 5-Hydroxymethylfurfural to 2,5-Furandicarboxylic Acid. *ChemSusChem* **2018**, *11*, 2083–2090. [[CrossRef](#)]
84. Nie, J.; Xie, J.; Liu, H. Activated carbon-supported ruthenium as an efficient catalyst for selective aerobic oxidation of 5-hydroxymethylfurfural to 2,5-diformylfuran. *Chin. J. Catal.* **2013**, *34*, 871–875. [[CrossRef](#)]
85. Artz, J.; Mallmann, S.; Palkovits, R. Selective Aerobic Oxidation of HMF to 2,5-Diformylfuran on Covalent Triazine Frameworks-Supported Ru Catalysts. *ChemSusChem* **2015**, *8*, 672–679. [[CrossRef](#)] [[PubMed](#)]
86. Vuyyuru, K.R.; Strasser, P. Oxidation of biomass derived 5-hydroxymethylfurfural using heterogeneous and electrochemical catalysis. *Catal. Today* **2012**, *195*, 144–154. [[CrossRef](#)]
87. Schade, O.R.; Kalz, K.F.; Neukum, D.; Kleist, W.; Grunwaldt, J.-D. Supported gold- and silver-based catalysts for the selective aerobic oxidation of 5-(hydroxymethyl)furfural to 2,5-furandicarboxylic acid and 5-hydroxymethyl-2-furancarboxylic acid. *Green Chem.* **2018**, *20*, 3530–3541. [[CrossRef](#)]
88. Zhang, Z.; Deng, K. Recent advances in the catalytic synthesis of 2,5-furandicarboxylic acid and its derivatives. *ACS Catal.* **2015**, *5*, 6529–6544. [[CrossRef](#)]
89. Saha, B.; Gupta, D.; Abu-Omar, M.M.; Modak, A.; Bhaumik, A. Porphyrin-based porous organic polymer-supported iron (III) catalyst for efficient aerobic oxidation of 5-hydroxymethyl-furfural into 2,5-furandicarboxylic acid. *J. Catal.* **2013**, *299*, 316–320. [[CrossRef](#)]
90. Gao, L.; Deng, K.; Zheng, J.; Liu, B.; Zhang, Z. Efficient oxidation of biomass derived 5-hydroxymethylfurfural into 2,5-furandicarboxylic acid catalyzed by Merrifield resin supported cobalt porphyrin. *Chem. Eng. J.* **2015**, *270*, 444–449. [[CrossRef](#)]
91. Jain, A.; Jonnalagadda, S.C.; Ramanujachary, K.V.; Mugweru, A. Selective oxidation of 5-hydroxymethyl-2-furfural to furan-2,5-dicarboxylic acid over spinel mixed metal oxide catalyst. *Catal. Commun.* **2015**, *58*, 179–182. [[CrossRef](#)]
92. Wang, S.; Zhang, Z.; Liu, B. Catalytic Conversion of Fructose and 5-Hydroxymethylfurfural into 2,5-Furandicarboxylic Acid over a Recyclable Fe₃O₄-CoO_x Magnetite Nanocatalyst. *ACS Sustain. Chem. Eng.* **2015**, *3*, 406–412. [[CrossRef](#)]

93. Yan, D.; Xin, J.; Shi, C.; Lu, X.; Ni, L.; Wang, G.; Zhang, S. Base-free conversion of 5-hydroxymethylfurfural to 2,5-furandicarboxylic acid in ionic liquids. *Chem. Eng. J.* **2017**, *323*, 473–482. [[CrossRef](#)]
94. Yan, D.; Xin, J.; Zhao, Q.; Gao, K.; Lu, X.; Wang, G.; Zhang, S. Fe–Zr–O catalyzed base-free aerobic oxidation of 5-HMF to 2,5-FDCA as a bio-based polyester monomer. *Catal. Sci. Technol.* **2018**, *8*, 164–175. [[CrossRef](#)]
95. Hayashi, E.; Komanoya, T.; Kamata, K.; Hara, M. Heterogeneously-Catalyzed Aerobic Oxidation of 5-Hydroxymethylfurfural to 2,5-Furandicarboxylic Acid with MnO₂. *ChemSusChem* **2017**, *10*, 654–658. [[CrossRef](#)] [[PubMed](#)]
96. Bao, L.; Sun, F.-Z.; Zhang, G.-Y.; Hu, T.-L. Aerobic Oxidation of 5-Hydroxymethylfurfural to 2,5-Furandicarboxylic Acid over Holey 2D Mn₂O₃ Nanoflakes from a Mn-based MOF. *ChemSusChem* **2019**. [[CrossRef](#)] [[PubMed](#)]
97. Han, X.; Li, C.; Liu, X.; Xia, Q.; Wang, Y. Selective oxidation of 5-hydroxymethylfurfural to 2,5-furandicarboxylic acid over MnOx–CeO₂ composite catalysts. *Green Chem.* **2017**, *19*, 996–1004. [[CrossRef](#)]
98. Zhang, S.; Sun, X.; Zheng, Z.; Zhang, L. Nanoscale center-hollowed hexagon MnCo₂O₄ spinel catalyzed aerobic oxidation of 5-hydroxymethylfurfural to 2,5-furandicarboxylic acid. *Catal. Commun.* **2018**, *113*, 19–22. [[CrossRef](#)]
99. Gao, T.; Yin, Y.; Zhu, G.; Cao, Q.; Fang, W. Co₃O₄ NPs decorated Mn-Co-O solid solution as highly selective catalyst for aerobic base-free oxidation of 5-HMF to 2,5-FDCA in water. *Catal. Today* **2019**. [[CrossRef](#)]
100. Neațu, F.; Marin, R.S.; Florea, M.; Petrea, N.; Pavel, O.D.; Pârvulescu, V.I. Selective oxidation of 5-hydroxymethyl furfural over non-precious metal heterogeneous catalysts. *Appl. Catal. B Environ.* **2016**, *180*, 751–757. [[CrossRef](#)]
101. Hayashi, E.; Yamaguchi, Y.; Kamata, K.; Tsunoda, N.; Kumagai, Y.; Oba, F.; Hara, M. Effect of MnO₂ Crystal Structure on Aerobic Oxidation of 5-Hydroxymethylfurfural to 2,5-Furandicarboxylic Acid. *J. Am. Chem. Soc.* **2019**, *141*, 890–900. [[CrossRef](#)]
102. Weckhuysen, B.M. Preface: Recent advances in the in-situ characterization of heterogeneous catalysts. *Chem. Soc. Rev.* **2010**, *39*, 4557–4559. [[CrossRef](#)]



© 2020 by the authors. Licensee MDPI, Basel, Switzerland. This article is an open access article distributed under the terms and conditions of the Creative Commons Attribution (CC BY) license (<http://creativecommons.org/licenses/by/4.0/>).